molecular pharmaceutics

Article

Cite This: Mol. Pharmaceutics 2019, 16, 4319−4338

pubs.acs.org/molecularpharmaceutics

Studying Excipient Modulated Physical Stability and Viscosity of Monoclonal Antibody Formulations Using Small-Angle Scattering

Amy Yuanyuan Xu,[†,‡] Maria Monica Castellanos,[†,‡,§] Kevin Mattison,[¶] Susan Krueger,[†] and Joseph E. Curtis*[,†]

[†]NIST Center for Neutron Research, National Institute of Standards and Technology, 100 Bureau Drive, Mail Stop 6102, Gaithersburg, Maryland 20899, United States

[‡]Institute for Bioscience and Biotechnology Research, University of Maryland, 9600 Gudelsky Drive, Rockville, Maryland 20850, United States

[¶]Malvern Panalytical, 117 Flanders Road, Westborough, Massachusetts 01581, United States

Supporting Information

ABSTRACT: Excipients are substances that are added to therapeutic products to improve stability, bioavailability, and manufacturability. Undesirable protein−protein interactions (PPI) can lead to self-association and/or high solution viscosity in concentrated protein formulations that are typically greater than 50 mg/mL. Therefore, understanding the effects of excipients on nonspecific PPI is important for more efficient formulation development. In this study, we used National Institute of Standards and Technology monoclonal antibody (NISTmAb) reference material as a model antibody protein to examine the physical stability and viscosity of concentrated formulations using a series of excipients, by varying pH, salt composition, and the presence of cosolutes including amino acids, sugars, and nonionic surfactants. Small angle X-ray scattering (SAXS) together with differential scanning calorimetry (DSC), dynamic light scattering (DLS), and viscosity measurements were used to obtain various experimental parameters to characterize excipient modulated PPI and bulk solution viscosities. In particular, a good correlation was found between SAXS and DLS/SLS results, suggesting that the use of DLS/SLS is valid for predicting the colloidal stability of NISTmAb in concentrated solutions. Moreover, further analysis of effective structure factor $S(q)_{eff}$ measured from SAXS enabled the dissection of net PPI into hydrodynamic forces due to excluded volume as well as any additional attractive or repulsive interactions with the presence of excipients. It was found that although no denaturation or aggregation of NISTmAb was observed and that the net PPI were repulsive, the use of ionic excipients such as pH and salts leads to increased short-range attraction, whereas the nonionic excipients including sugars, amino acids, and polysorbate surfactants lead to increased repulsive PPI with increasing protein concentration. Results obtained from viscosity measurements showed that the use of excipients can lead to increased solution viscosities at high protein concentrations. The use of $S(q)_{eff}$, interaction parameter k_D, and second virial coefficient B_{22} as predictors for solution viscosity was also evaluated by comparing the predicted results with the measured viscosities. Although B_{22} and $S(q)_{eff}$ appeared to be better predictors than k_D, disagreement between the predicted and measured results suggests other factors apart from PPI contribute to the bulk rheological properties of concentrated protein solutions.

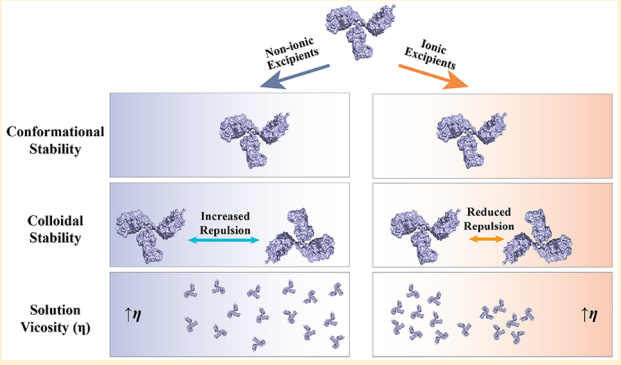

KEYWORDS: *monoclonal antibodies, formulation, excipient, protein−protein interactions, physical stability, viscosity, small angle scattering, dynamic light scattering*

INTRODUCTION

One of the challenges of biopharmaceutical research and development is the physical instability of therapeutic proteins in solution, as this could lead to protein denaturation or aggregation, which can compromise the efficacy and safety of the therapeutic products. Physical instability of proteins can be divided into two major categories: conformational instability, which refers to the conformational changes from native to non-native states, and colloidal instability, which is reflected by the protein's propensity to self-associate. The conformation of proteins is maintained through noncovalent bonds between atoms in the polypeptide backbone as well as those in the amino acid side chains. Environmental factors such as pH and temperature can have negative impacts on the conformational stability of proteins. Colloidal stability, on the other hand, is

Received: June 24, 2019
Revised: September 4, 2019
Accepted: September 5, 2019
Published: September 5, 2019

DOI: 10.1021/acs.molpharmaceut.9b00687
Mol. Pharmaceutics 2019, 16, 4319−4338

controlled by the balance between attractive and repulsive interactions among proteins and other molecules in solution; these interactions include hydrogen bonding, electrostatic, and hydrophobic forces.[1]

Concentrations greater than 50 mg/mL can be required to meet the desired therapeutic doses for protein therapeutics, such as monoclonal antibodies (mAbs).[2,3] As a consequence of increased protein concentration, solution viscosities may be elevated significantly (greater than 50 cP), causing difficulties in product development and the subcutaneous injection of protein therapeutics.[4,5] Moreover, at high protein concentrations, the average distance between individual protein molecules can be significantly reduced, from a few to tens of nanometers.[6−8] As a result, the nonspecific protein−protein interactions (PPI), such as hydrophobic, electrostatic, van der Waals, and dipole−dipole interactions, become more significant. Protein aggregation resulting from undesirable PPI represents one of the major challenges in formulation development, as protein aggregates can lead to the loss of therapeutic effects and induce harmful immune responses.[9,10] Therefore, excipients are frequently used to improve the physical stability of therapeutic protein formulations.[11−13] Common examples include buffering species to modulate solution pH, surfactants to inhibit protein adsorption to interfaces, and cosolvents such as salts, sugars, and amino acids to stabilize proteins and to obtain physiological tonicity and osmolality.[14] The mechanisms through which proteins are stabilized vary among different excipient classes: some excipients stabilize proteins through direct interactions, whereas others preferentially interact with solvents or interfaces that then indirectly stabilize the proteins.[11,13] In either case, proteins are generally expected to be stabilized if the net PPI are repulsive.[15]

Great effort has been made to the characterization of physicochemical properties of proteins in a wide variety of excipient conditions with the aid of high-throughput screening techniques including differential scanning fluorimetry (DSF), differential scanning calorimetry (DSC), size exclusion chromatography (SEC), static light scattering (SLS), and dynamic light scattering (DLS).[12,13,16−19] Conformational stability of proteins can be expressed as their resistance to thermal unfolding.[2] In practice, DSC measurements are most commonly performed to obtain the melting temperature T_m of proteins under various excipient conditions; the higher the T_m, the greater the conformational stability against thermal or chemical unfolding. Influenced by various attractive and repulsive interactions between different molecules, colloidal stability of proteins is reflected by their tendency to remain in monomeric form. Multiple techniques have been used to predict the long-term colloidal stability of proteins in concentrated formulations; the most frequently used techniques are SLS and DLS, from which the osmotic second virial coefficient B_{22} and diffusion interaction parameter k_D are estimated from the nonideal solution behavior in dilute protein solutions (<20 mg/mL).[20,21] Because both k_D and B_{22} contain information on nonspecific PPI, they are also used as predictors of viscosity for highly concentrated protein formulations.[16,22−26] Recently, there is a growing concern about the suitable use of k_D and B_{22} to study concentrated formulations, as they are measures of dilute solution properties.[15,27] It is anticipated that at high concentrations, the elevated crowding effects can have significant impacts on the PPI when averaged over many neighboring molecules.[27−29] Moreover, because both k_D and B_{22} are measured from dilute samples, they may not provide accurate predictions on solution viscosities that do not manifest until much higher concentrations.[15,22,27] Small angle scattering with either X-rays (SAXS) or neutrons (SANS) represents one of the few biophysical characterization techniques where PPI can be directly quantified from concentrated formulations.[30−34] Scattering measurements can be performed on both dilute and concentrated samples (from a few to hundreds of mg/mL), to obtain experimental parameters of form factor $P(q)$ and effective structure factor $S(q)_{eff}$, respectively. $P(q)$ is predominate in dilute solutions and contains information on the size and shape of protein molecules, whereas $S(q)_{eff}$ also contributes toward the total scattering with increasing protein concentrations, as it describes the spatial arrangements and intermolecular interactions of protein molecules in concentrated systems. Traditionally, SAXS is largely used to determine the conformation of biomacromolecules, because it provides measures of $P(q)$. In this study, we show that $S(q)_{eff}$ can be utilized for studying excipient modulated physical stability and viscosity of monoclonal antibody formulations.[34] SAXS can be a valuable technique for high-throughput formulation development.

In this study, we used the National Institute of Standards and Technology (NIST) monoclonal antibody reference material (NISTmAb) as a model antibody protein to study the effects of five different classes of excipients on the physical stability and viscosity of antibody formulations. NISTmAb is a humanized IgG1κ mAb (RM 8670) that can be considered as a typical biopharmaceutical product whose structure and stability have been extensively characterized.[35,36] NISTmAb solution prepared in 25 mM histidine buffer was considered as the control sample, and the physical stability and viscosity of various formulations were investigated by studying the changes in experimental parameters with and without the presence of excipients. DSC, DLS/SLS, SAXS, and viscometry experiments were performed to obtain values of T_m, k_D, B_{22}, $S(q)_{eff}$, and viscosity (η) from different samples. In particular, the physical stability of NISTmAb in various formulations was studied by experimental parameters measured from both dilute (k_D, B_{22}) and concentrated ($S(q)_{eff}$) solutions. Results from these data sets were compared, and the use of k_D and B_{22} for studying concentrated protein formulations was evaluated. Moreover, the use of k_D, B_{22}, and $S(q)_{eff}$ as predictors for η was evaluated by comparing the predicted results with experimentally determined η. Lastly, this study provides extensive information on the physical stability and viscosity of NISTmAb formulations; the effects of various excipients on NISTmAb were also compared with other proteins. Together, these results will be beneficial for the development of a more efficient formulation design methodology.

EXPERIMENTAL METHODS

Certain commercial equipment, instruments, or materials (or suppliers, or software, ...) are identified in this paper to foster understanding. Such identification does not imply recommendation or endorsement by the National Institute of Standards and Technology nor does it imply that the materials or equipment identified are necessarily the best available for the purpose. NISTmAb reference material (RM 8670) was received as 10 and 100 mg/mL protein solutions prepared in 25 mM histidine buffer at pH 6. L-Histidine and L-histidine chloride were used to prepare additional pH 6, 25 mM histidine buffer.[36] In order to prepare NISTmAb in different formulation conditions, excipient solutions were first prepared by adding appropriate amount of excipients to 25 mM histidine buffer at

DOI: 10.1021/acs.molpharmaceut.9b00687
Mol. Pharmaceutics 2019, 16, 4319−4338

Table 1. List of Excipient Conditions Examined in This Study[a]

excipients	buffer	ionic concentration (mM)	pH
300 mM sucrose	25 mM histidine	12.5	6
300 mM trehalose	25 mM histidine	12.5	6
300 mM glucose	25 mM histidine	12.5	6
237 mM mannitol	25 mM histidine	12.5	6
171 mM arginine	25 mM histidine	196	6
200 mM proline	25 mM histidine	12.5	6
200 mM glycine	25 mM histidine	12.5	6
200 mM alanine	25 mM histidine	12.5	6
0.120 mM polysorbate 80	25 mM histidine	12.5	6
0.0600 mM polysorbate 20	25 mM histidine	12.5	6
150 mM NH_4Cl	25 mM histidine	163	6
150 mM Na_2SO_4	25 mM histidine	313	6
150 mM NaCl	25 mM histidine	163	6
150 mM $NaClO_4$	25 mM histidine	163	6
-	67 mM phosphate	82.8	6
-	67 mM phosphate	148	7
-	67 mM phosphate	196	8

[a]The unit M stands for the molar concentration of mol/L, whereas mM stands for the concentration of 10^{-3} mol/L.

pH 6 to reach desired concentrations. Excipients used in this study include sugars: sucrose, glucose, trehalose, mannitol; salts: NaCl, NH_4Cl, Na_2SO_4, $NaClO_4$; amino acids: arginine, proline, alanine, glycine; and surfactants: polysorbate 20 and 80. After excipients were fully dissolved, the pH of each solution was checked and adjusted to pH 6. Excipient solutions were then filtered through 0.22 μm filter prior to further use. NISTmAb in the original formulation buffer was loaded into the Amicon Ultra-15 centrifugal filters with membranes with a molecular weight cutoff of 30 kDa, and the buffer background of NISTmAb was exchanged six times with the desired excipient solution. Concentrations of NISTmAb solutions were measured by a NanoDrop UV−vis spectrometer (ND-2000, Thermal Scientific, Wilmington, US) using a theoretical extinction coefficient of 1.42 mL mg^{-1} cm^{-1}.[37] For each excipient condition, a series of NISTmAb solutions were prepared to cover protein concentrations from 1−170 mg/mL. Other chemicals used in this study were of analytical grade and used without further purification. Protein samples were stored at 4 °C and measured within 3 days after preparation. Molar concentrations of excipients (except surfactants) were used in this study, because it is generally considered that high excipient concentrations are required to achieve long-term protein stability and to balance the osmolality of the high-protein-concentration formulations.[13] Concentrations used for polysorbate 20 (P20) and polysorbate 80 (P80) were chosen based on their proven abilities to stabilize proteins against aggregation; the selected concentrations for P20 and P80 were above their critical micelle concentrations (55 and 13 μM, respectively).[38,39] Also, in order to characterize the effects of solution pH on the physical stability of NISTmAb, phosphate salts were used to prepare solutions with pH values of 6, 7, and 8.

Dynamic and Static Light Scattering. DLS was measured at 25 °C using a Zetasizer Nano ZSP system (Malvern Panalytical, Malvern, UK) with a scattering angle of 173°. In a DLS experiment, the time-dependent fluctuations of the particle are analyzed using an autocorrelator, through which an autocorrelation function is generated. The correlation signal G decays at an exponential rate and is dependent on the translational diffusion coefficient of the particle[40] (eq 1)

$$G = \int_0^\infty I(t)I(t+\tau)\mathrm{d}t = B + A\mathrm{e}^{-2Dq^2\tau} \quad (1)$$

where B is the background term, A is the instrument-dependent optical constant, and D is the diffusion coefficient. In sufficiently dilute systems, the average hydrodynamic radius (R_H) of a particle can be calculated from its diffusion coefficient using the Stokes−Einstein equation (eq 2)

$$D = \frac{k_B T}{6\pi\eta R_H} \quad (2)$$

where k_B is the Boltzmann constant, T is the temperature, and η is the sample viscosity. It should be noted that the diffusion coefficient (D) measured by DLS is the mutual or collective diffusion coefficient. For concentrated systems, the nonspecific interactions between protein molecules become more significant, and they have a direct impact on the D value measured from DLS. Under such conditions, both thermodynamic (direct PPI) and hydrodynamic (frictional force) interactions contribute to the measured D_c value. The DLS interaction parameter k_D describes the dependence of the diffusion coefficient on particle concentration in a given medium. Experimentally, k_D can be determined as the linear slope of the D versus concentration dependence in the lower-concentration region (<20 mg/mL)[20,21] (eq 3)

$$D = D_0(1 + k_D C) \quad (3)$$

where D_0 is the self-diffusion coefficient of the particle and can be determined from the intercept of the D versus concentration (C) plot. The value of k_D has been used widely in the biopharmaceutical industry to predict the colloidal stability of proteins in various formulations. B_{22} is another measure of weak PPI resulting from nonideal solution behavior.[24] Experimentally, B_{22} can be determined as the slope of a Debye plot in the lower-protein-concentration regime

$$\frac{KC}{R_\theta} = \frac{1}{M_W} + 2B_{22}C \quad (4)$$

where K is the optical constant, R_θ is the Rayleigh ratio between the incident and scattered light intensity, and M_W is the average molar weight of the protein. A negative B_{22} value is indicative of net attractive PPI, whereas a positive value implies net repulsive PPI. Although both k_D and B_{22} can be used to predict the colloidal stability of proteins in solution, these two parameters are different, and the relationship between the two can be expressed as[41]

$$k_D = 2M_W B_{22} - (k_s + \nu) \quad (5)$$

where k_s represents the change in the sedimentation coefficient per unit change in concentration, and ν is the partial specific volume of the protein. Unlike B_{22}, k_D does not define attractive or repulsive PPI with values below or above precisely zero.

Electrophoretic Light Scattering. Electrophoretic light scattering (ELS) measurements were performed using a Zetasizer Nano ZSP system (Malvern Panalytical, Malvern, UK). ELS measures the Doppler shift (Δf) in the frequency of light scattering from charged particles moving under the influence of an applied electric field. The electrophoretic mobility (μ) is calculated from the Doppler shift

DOI: 10.1021/acs.molpharmaceut.9b00687
Mol. Pharmaceutics 2019, 16, 4319−4338

$$\Delta f = \frac{2\mu E}{\lambda}\sin\left(\frac{\theta}{2}\right) \quad (6)$$

where E is the applied field strength, λ is the incident light wavelength, and θ is the scattering angle. The zeta potential is the electrical potential at the hydrodynamic boundary or slipping plane (defined by the Stokes radius R_S), arising from the net surface charge of the particle (defined by the hard sphere radius α), and is used to predict the colloidal stability of charged particles in solution.[42,43] Experimentally, the zeta potential (ζ) is not measured directly but is calculated from the measured electrophoretic mobility using Henry's equation

$$\mu = \frac{2\varepsilon\zeta f(\kappa\alpha)}{3\eta} \quad (7)$$

where ε is the dielectric constant of the dispersant, $f(\kappa\alpha)$ is Henry's function, and η is the viscosity.[43] In this study, $f(\kappa\alpha)$ is approximated to 1.5 according to the Smoluchowski approximation,[42,43] as it was assumed that the thickness of the electrical double layer is much thinner than the particle radius. In order to determine the zeta potential of NISTmAb, the electrophoretic mobility of the protein was measured at 10 mg/mL solution in various excipient conditions.

Small Angle X-ray Scattering. SAXS measurements were made at 25 °C on a custom-built SAXSLab Ganesha SAXS instrument coupled with a Rigaku MicroMax-007 HF rotating anode generator. Protein solutions were loaded into a sealed 96-well plate, and 20 μL of each sample was transferred into a 1.3 mm capillary for X-ray exposure. Two configurations were used to cover a q range of 0.005−0.45 Å^{-1}, where q, the scattering vector, is defined as

$$q = \frac{4\pi}{\lambda}\sin(\theta) \quad (8)$$

In a SAXS experiment, a well-collimated X-ray beam is used to illuminate the sample with the angle-dependent scattering intensity recorded at the detector. A scattering profile of a particular system is typically represented as the double logarithm plot of the scattering intensity $I(q)$ as a function of the scattering vector q. For a simple, noncompressible system consisting of monodisperse scattering particles in solvent, $I(q)$ on an absolute scale can be modeled as

$$I(q) = \frac{N}{V}(\Delta\rho)^2 V_P^2 P(q) S(q) \quad (9)$$

where (N/V) is the number density of the particles, $\Delta\rho$ is the difference in the scattering length density between the particles and the solvent background, and V_P refers to the particle volume. In addition, $P(q)$ is the form factor that represents the shape of the scattering objects, and $S(q)$ is the structure factor that reflects the interparticle contributions to $I(q)$ and is unity at low particle concentrations where the interparticle interference is negligible. SAXS data collection and reduction were performed using the software package BioXTAS RAW.[44] The radius of gyration (R_g) of NISTmAb was calculated using Guinier approximation[45]

$$\ln(I(q)) = \ln(I(0)) - \left(\frac{R_g^2}{3}\right)q^2 \quad (10)$$

where $I(0)$ represents the scattering intensity at zero angle. SAXS experiments were performed on a series of NISTmAb concentrations for each excipient formulation. At lower protein concentrations, the scattering profiles were dominated by the $P(q)$ of NISTmAb, and protein molecules were separated from each other with negligible PPI. Nonspecific PPI became more significant in a crowded environment; as a result, SAXS profiles measured at higher protein concentrations reflected contributions from both $P(q)$ and $S(q)$. Compared to the SAXS profiles measured from dilute solutions where PPI were minimal, the appearance of $S(q)$ was reflected by the deviation of $I(q)$ at a low scattering angle. Scattering profiles measured from 6 mg/mL NISTmAb solutions were subjected to Guinier analysis, because the interparticle interference (i.e., nonspecific PPI) was negligible at these dilute concentrations.[33,34,46] The $S(q)_{eff}$ of NISTmAb was determined by division of $I(q)$ by $P(q)$ for concentrated samples. Here, the experimentally determined structure factor is defined as "effective" $S(q)$ (i.e., $S(q)_{eff}$), because it is affected by the shape and anisotropy of interactions between molecules.[47] To take the configurational flexibility of an antibody protein into account, ensembles of atomistic structures were obtained using SASSIE[48] by sampling the backbone dihedral angles of the hinge region in a Monte Carlo simulation.[49,50] The $P(q)$ of the ensembles was then calculated from the atomistic coordinates using the Xtal2Sas module, which is also available from SASSIE.[48,51,52] Ensembles of $S(q)_{eff}$ were calculated from experimental total scattering $I(q)$ and collections of $P(q)$ (including the one measured from 6 mg/mL protein solution and those derived from ensembles) by solving eq 9.

$S(q)_{eff}$ is concentration-dependent and accounts for both the excluded volume effect as well as any additional repulsive or attractive interactions between molecules.[34,53] An $S(q)_{eff}$ value of unity suggests the PPI are negligible, whereas a value less than unity is indicative of net repulsive PPI and vice versa. Experimental $S(q)_{eff}$ were analyzed using Ornstein−Zernike (OZ) integral equation with the assumption that the protein molecules are spherical particles. Percus−Yevick (PY) closure was used for the calculation of $S(q)_{eff}$ using a hard sphere model where the excluded volume was considered to be the only interaction.[32] The interparticle potential $U(r)$ can be expressed as[54]

$$U(r) = \begin{cases} \infty, & r < 2R \\ 0, & r \geq 2R \end{cases} \quad (11)$$

where r is the distance from the center of the sphere of a radius R. Two parameters were involved in the fitting process of the hard sphere model: volume fraction and radius of proteins. Because the volume fraction was known, the radius was fitted within constraints (3.9−5.5 nm). Accounting for additional Coulomb repulsion between macromolecules, a Hayter−Penfold model was also used to model $S(q)_{eff}$. The interaction potential $U(r)$ of charged particles can be expressed as[55]

$$U(r) = \begin{cases} \dfrac{Z^2}{\pi\epsilon_0\epsilon(2+\kappa\delta)^2}\dfrac{e^{-\kappa(r-\delta)}}{r}, & r \geq \delta \\ \infty, & r < \delta \end{cases} \quad (12)$$

where Z is the effective charge, δ is the effective diameter, κ is the inverse of the Debye−Huckel screening length, ϵ_0 is the permittivity of free vacuum, and ϵ is the dielectric constant of the solvent. When both attractive and repulsive interactions were present, a two-Yukawa model was used to model $S(q)_{eff}$ instead.[56] The reduced interaction potential $U(x)$ is expressed as[57]

DOI: 10.1021/acs.molpharmaceut.9b00687
Mol. Pharmaceutics 2019, 16, 4319−4338

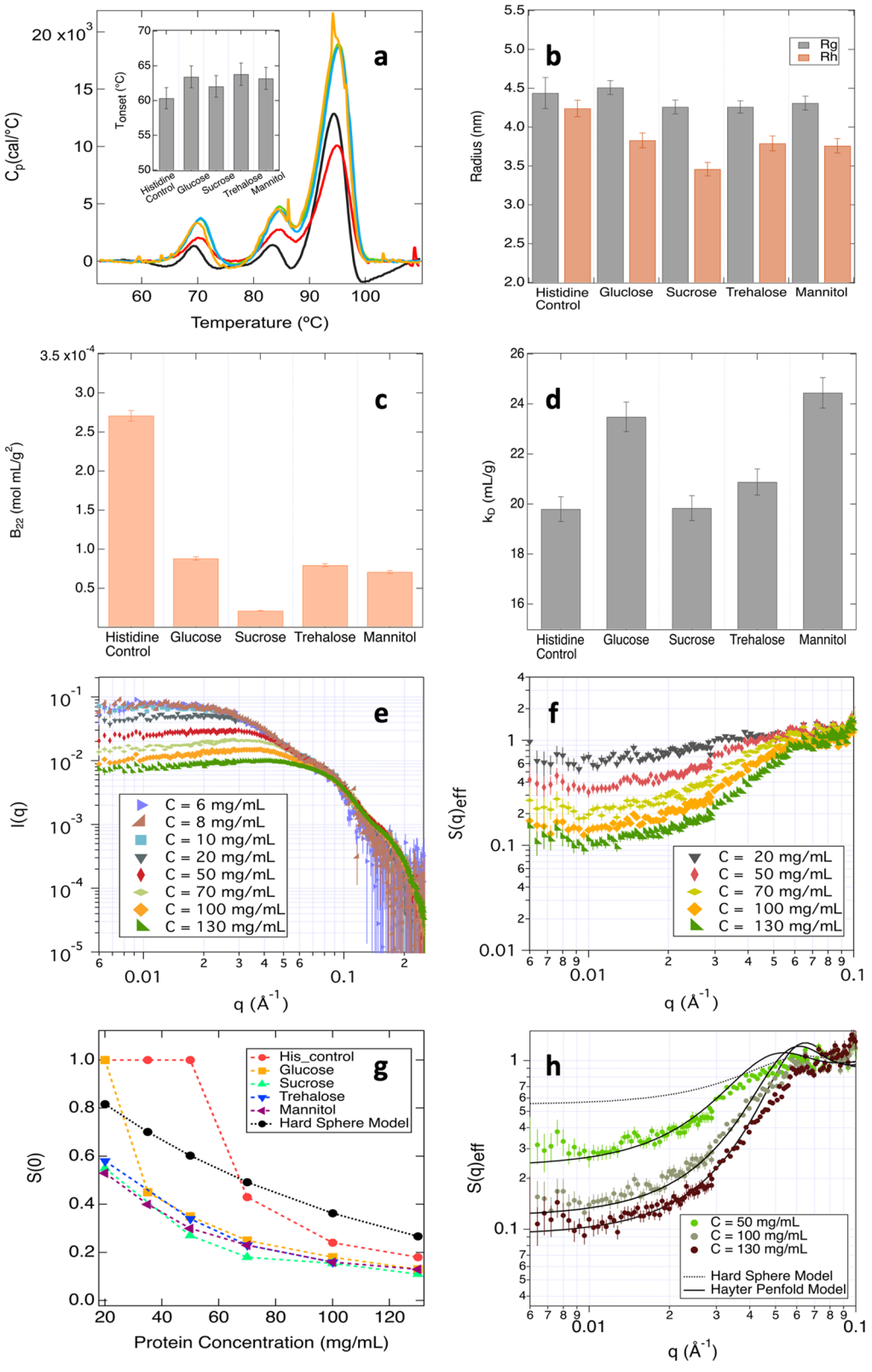

Figure 1. (a) DSC thermograms and T_{onset} (inset) measured from NISTmAb formulations with sugar excipients. Data sets are colored as histidine control (black), glucose (red), mannitol (orange), sucrose (green), and trehalose (blue). (b) R_g (gray colored) and R_H (orange colored) of NISTmAb in various excipient conditions. R_g was calculated using the ATSAS Primus software package.[71,72] (c,d) B_{22} and k_D values calculated from histidine control and sugar excipient formulations. (e) SAXS profiles measured from NISTmAb in sucrose solution with a protein concentration ranging from 6−130 mg/mL. (f) $S(q)_{eff}$ of NISTmAb in sucrose solution as a function of protein concentration. (g) Summary of $S(0)_{exp}$ at $q \rightarrow 0$ measured from a histidine control as well as four sugar excipient formulations; $S(0)_{HS}$ derived from a hard sphere model is also presented for comparison. Dotted lines are drawn to guide the eye. (h) $S(q)_{eff}$ measured from 50, 100, and 130 mg/mL of NISTmAb in sucrose solution. Dotted and solid lines represent the fit

DOI: 10.1021/acs.molpharmaceut.9b00687
Mol. Pharmaceutics 2019, 16, 4319−4338

Figure 1. continued

from the hard sphere (for 50 mg/mL sample) and Hayter−Penfold (for 50, 100, and 130 mg/mL samples) models, respectively. Errors in (a−d) correspond to 1 standard deviation.

$$U(x) = \begin{cases} -K_1\frac{e^{-Z_1(x-1)}}{x} - K_2\frac{e^{-Z_2(x-1)}}{x}, & x \geq 1 \\ \infty, & x < 1 \end{cases} \quad (13)$$

where x equals to r/δ, K_1 and Z_1 are the strength and range of attraction, respectively, and K_2 and Z_2 are the strength and range of repulsion, respectively. Data analysis was performed using an NCNR analysis macro built into IgorPro.[58] The magnitude of $S(q)_{eff}$ was represented by $S(0)_{exp}$ at infinite low q (i.e., when q was approaching zero). Values of $S(0)_{exp}$ were obtained by fitting the $S(q)_{eff}$ profiles using appropriate models.

Microcapillary Viscometry. The viscosities η of NISTmAb formulations were measured in duplicate using a Viscosizer TDA system (Malvern Panalytical, Malvern, UK) at 25 °C. During a viscosity measurement, sample flows through a 75 μm ID hydroxypropyl cellulose coated microcapillary with two detection windows at constant driving pressure. Therefore, the shear rate is dependent upon the solution viscosity and the applied pressure according to Poiseuille's Law[59]

$$Q = \frac{\pi r^4 \Delta P}{8\eta L} \quad (14)$$

where r and L are the radius and length of the capillary, respectively. For example, the shear rate measured from NISTmAb in 25 mM histidine buffer ranges from 1300 s^{-1} (measured at 10 mg/mL protein concentration) to 210 s^{-1} (measured at 170 mg/mL protein concentration). The travel time between the two windows (Δt_S) is recorded and used to calculate the relative viscosity of the sample (η_{rel}) using eq 15.

$$\eta_{rel} = \left(\frac{2L}{l_1 + l_2}\right)\left(\frac{\Delta t_S - \Delta t_B}{\Delta t_B}\right) + 1 = \frac{\eta_S}{\eta_B} \quad (15)$$

where l_1 and l_2 are the positions of windows 1 and 2 along the capillary, respectively, and Δt_S and Δt_B are the flow time of the sample and buffer, respectively. The buffer viscosity was measured using water as a reference and then used to calculate the sample viscosity (eq 15). Size measurements were collected before and after triplicate viscosity measurements to confirm the absence of coating degradation and protein−capillary wall interactions, which would be evident in a broadening of the trailing edge during a size measurement.

Differential Scanning Calorimetry. Differential scanning calorimetry experiments were performed using a MicroCal VP-DSC instrument (Malvern Panalytical, Malvern, UK). Both sample and buffer solutions were degassed under vacuum for 7 min with constant stirring prior to measurement. Changes in heat capacity were recorded from 50−110 °C for each sample. DSC thermograms of protein samples were corrected by subtracting the buffer−buffer baseline. The onset temperature (T_{onset}) is defined as the temperature at which significant changes in heat capacity are first observed, and it has been used as one of the parameters to assess protein thermal stabilities.[60−63] Because multiple transitions (attributed to various segments of mAbs) were observed as temperature increased, we used T_{onset} to assess the melting temperature of NISTmAb in different excipient formulations. In order to avoid possible contribution from instrument sensitivity and protein concentrations to the melting temperature, all the samples were measured at the same concentration on the same instrument.

RESULTS

Sugars as Excipients. Sugars are commonly used excipients to formulate protein therapeutics.[5] In this study, four different sugars were chosen to study their effects on the physical stability and viscosity of NISTmAb formulations; these include glucose (a monosaccharide), sucrose and trehalose (disaccharides), and mannitol (a sugar alcohol). Although sucrose, trehalose, and mannitol are frequently used excipients for antibody formulations, glucose is less commonly used, because it is a reducing sugar, which could lead to undesired glycation of proteins and subsequent aggregation.[64,65] Glucose was included in this study to compare the stabilizing effects of monosaccharide and disaccharides.

The conformational stability of NISTmAb was studied by DSC with and without the addition of sugar excipients (Figure 1a). DSC scans resolved three unfolding transitions comprising endothermic peaks, attributable to the unfolding of CH_2, CH_3, and eventually the Fab domain of NISTmAb.[37] Derived from the DSC thermogram, the values of T_{onset} were increased by ∼3 °C when sugars were added, suggesting the conformation of NISTmAb was stabilized under the studied excipient conditions. This is consistent with other studies where sugars demonstrate stabilizing effects to protein conformation in liquid formulations.[66−68] Despite the changes in the unfolding temperature, variations in R_H and R_g of NISTmAb were also measured to study NISTmAb's conformational stability. Both R_H and R_g were determined from 6 mg/mL protein solutions for comparison. Results shown in Figure 1b suggest that there was a considerable decrease in R_H, whereas the R_g values of NISTmAb remained constant when sugars were added. The reduced R_H values could be a consequence of altered intermolecular interactions between NISTmAbs, for example, an increase in electrostatic repulsion arising from a reduction in the solution dielectric constant upon sugar addition.[69] Another possible explanation for the observed reduction in R_H values is that sugar molecules were preferentially excluded from the protein surface, resulting in a more compact protein conformation on average.

The colloidal stability of NISTmAb was studied by both B_{22} and k_D measured from dilute formulations. Both the B_{22} and k_D values were positive (Figure 1c,d), suggesting the net PPI between NISTmAb molecules were repulsive. As compared to the histidine control, B_{22} values were reduced significantly, whereas the values of k_D either remained constant or increased considerably with the presence of sugar excipients. There are two principal physical contributions to B_{22}: electrostatic repulsion and excluded volume, with a reduction in either or both leading to a reduction in B_{22}. Given the low effective charge of NISTmAb at the pH employed in this study (pH 6),[31] the reduction in B_{22} upon sugar addition suggests a significant reduction in the excluded volume, a suggestion consistent with the observed increase in T_{onset} and decrease in R_H upon sugar addition. As previously mentioned, k_D is a result of both thermodynamic and hydrodynamic parameters; therefore, a

DOI: 10.1021/acs.molpharmaceut.9b00687
Mol. Pharmaceutics 2019, 16, 4319−4338

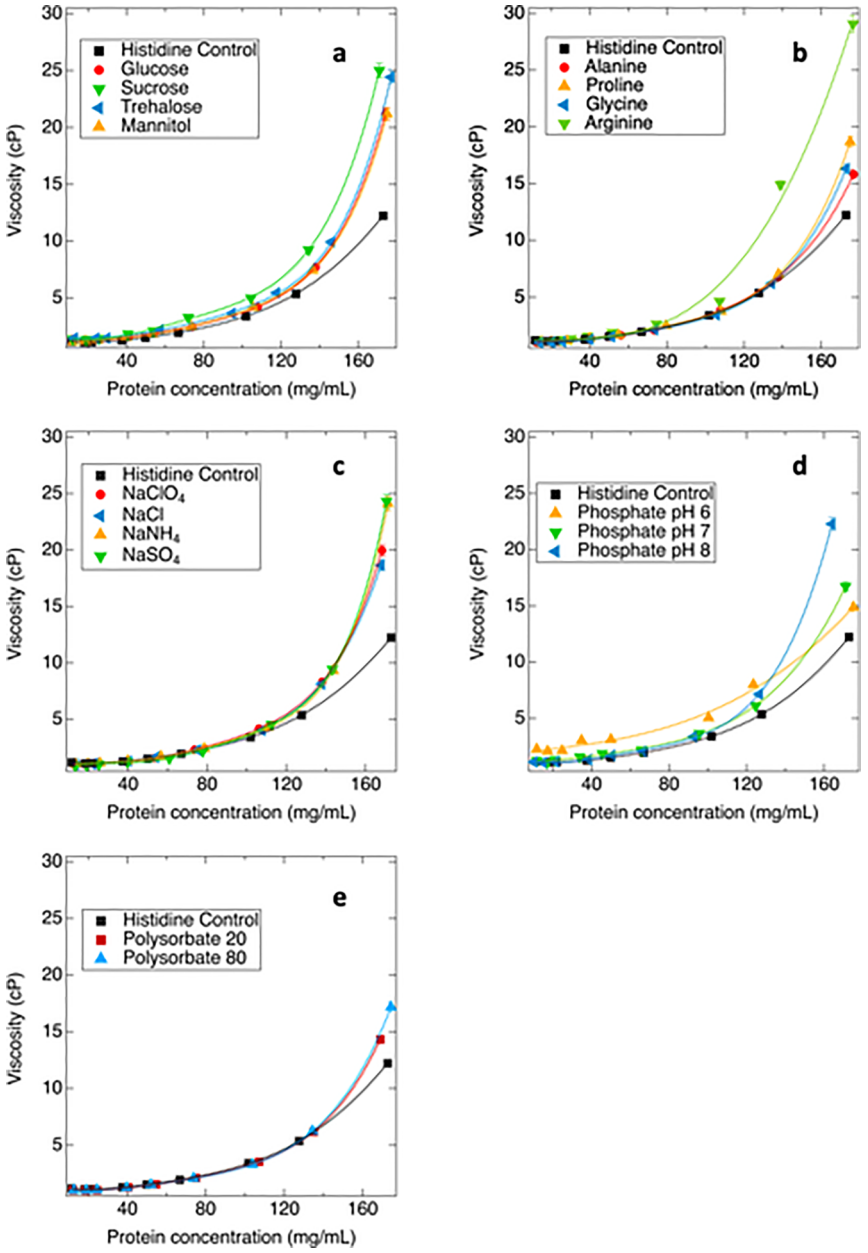

Figure 2. (a–e) η values of NISTmAb solutions measured from various sugar, amino acid, salt, pH, and surfactant excipient formulations. Errors correspond to standard deviations between two measurements.

constant or increased k_D value with a concomitant decrease in B_{22} is likely a result of increased hydrodynamic interactions that are solvent-mediated and dependent on solution viscosity, protein–solvent interactions, and so on.[28,70]

Example scattering profiles measured for the NISTmAb solutions with sucrose are shown in Figure 1e. SAXS profiles measured from all protein concentrations demonstrated similar behavior at the high-q region, where $q \leq 1/D$, and D is the diameter of NISTmAb molecule. Because $I(q)$ was dominated by $P(q)$ of proteins at high q, the overlap of scattering profiles in this q region confirmed the conformational stability of NISTmAb in concentrated sucrose solution. Although the scattering at high q remained constant, a decrease in $I(0)$ was observed starting from 20 mg/mL, and the deviation became more significant with increasing NISTmAb concentration. In order to further explore the PPI in concentrated protein solutions, $S(q)_{eff}$ was isolated from $I(q)$ and presented in Figure 1f.

Data in Figure 1f suggests that $S(q)_{eff}$ was less than unity with increasing protein concentrations; such a change in $S(q)_{eff}$ implied the presence of net repulsive PPI between NISTmAb molecules in sucrose solution. In order to assess the nature of interactions that together result in the observed $S(q)_{eff}$, different models were used to fit $S(q)_{eff}$ measured at various protein concentrations, including the hard sphere and Hayter–Penfold model as well as the two-Yukawa model. Theoretical $S(0)$ values calculated from hard sphere model ($S(0)_{HS}$) were summarized and compared with $S(0)_{exp}$ values in Figure 1g. In the case of the histidine control sample, $S(q)_{eff}$ was negligible until the protein concentration increased to 50 mg/mL. Beyond this concentration, $S(0)_{exp}$ became less than $S(0)_{HS}$, suggesting that repulsive interactions, rather than excluded volume effects, control the net repulsive PPI observed at higher protein

DOI: 10.1021/acs.molpharmaceut.9b00687
Mol. Pharmaceutics 2019, 16, 4319–4338

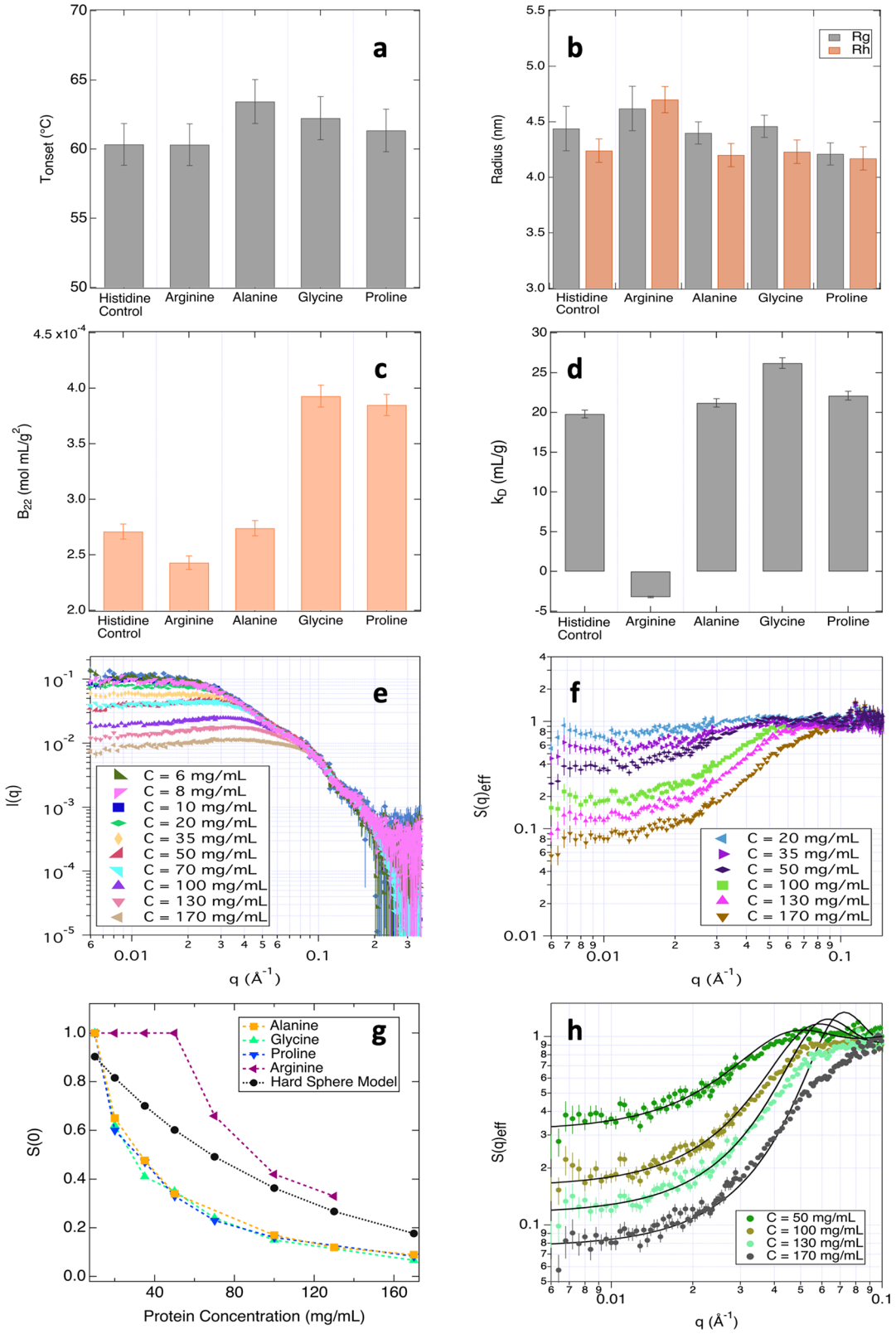

Figure 3. (a) Summary of T_{onset} measured of NISTmAb formulations with amino acid excipients. (b) R_g and R_H of NISTmAb in amino acid excipient conditions. (c,d) B_{22} and k_D calculated from NISTmAb solutions with and without amino acid excipients. (e) Summary of SAXS profiles measured from alanine excipient formulation. (f) $S(q)_{eff}$ of NISTmAb in alanine solution as a function of protein concentration. (g) Changes in $S(0)$ values as a function of protein concentration; dotted lines were drawn to guide the eye. (h) $S(q)_{eff}$ measured from arginine solution is best fit using a two-Yukawa model. Error values in (a−d) correspond to 1 standard deviation.

concentrations. For samples with sugar excipients, $S(0)_{exp}$ became less than unity at much lower protein concentrations: 35 mg/mL for glucose and 20 mg/mL for the rest. The values of $S(0)_{exp}$ were much less than the values of $S(0)_{HS}$ for all examined

DOI: 10.1021/acs.molpharmaceut.9b00687
Mol. Pharmaceutics 2019, 16, 4319−4338

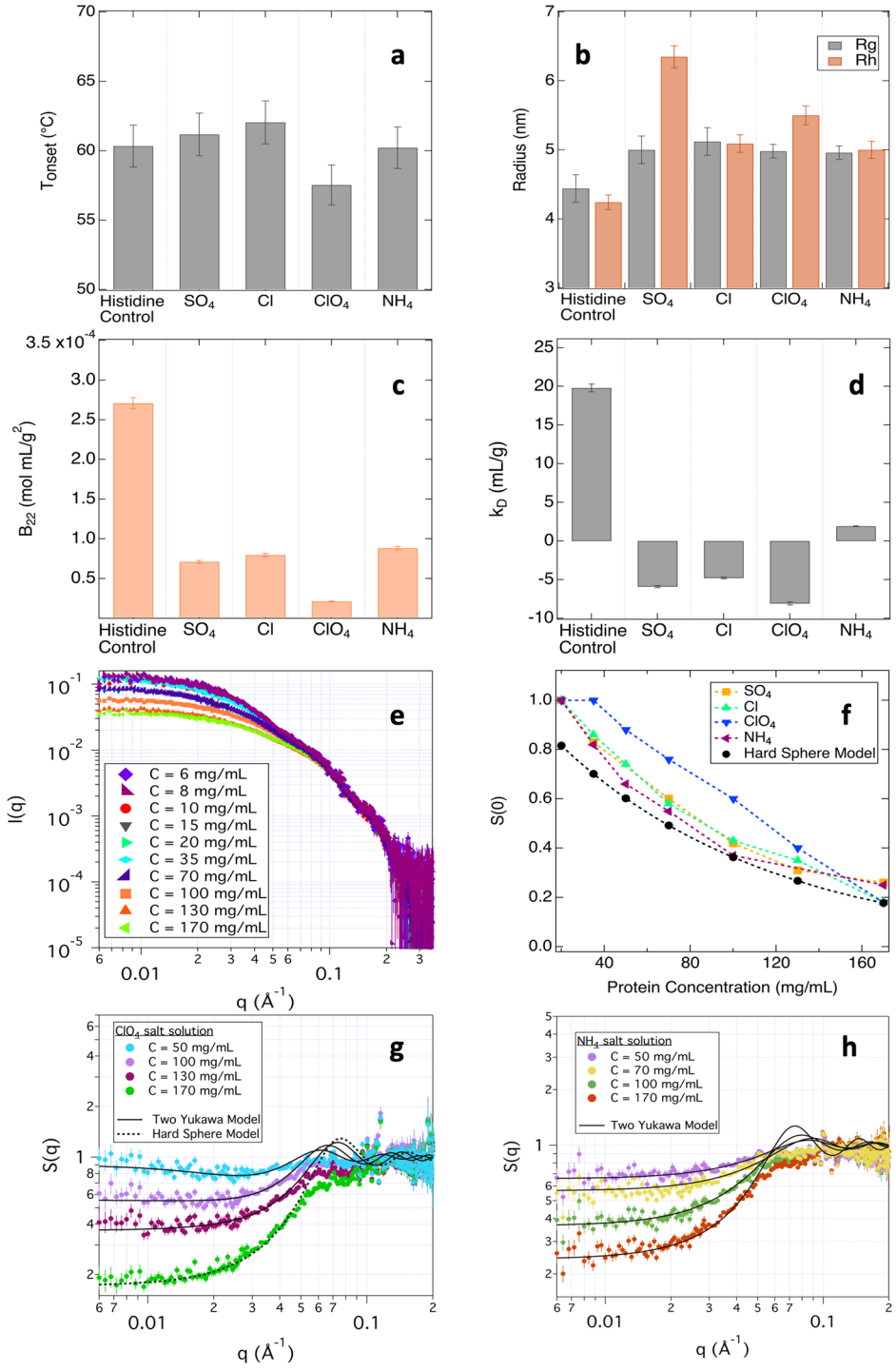

Figure 4. (a) Summary of T_{onset} of NISTmAb in various salt formulations. (b) R_g and R_H values of NISTmAb measured in salt solutions. (c,d) B_{22} and k_D values calculated from NISTmAb solutions with and without salt excipients. (e) Summary of SAXS profiles measured from perchlorate excipient formulation. (f) Changes in $S(0)_{exp}$ values as a function of protein concentration; dotted lines were drawn to guide the eye. (g) $S(q)_{eff}$ measured from perchlorate solution was best fit using a two-Yukawa model when protein concentration was between 50−130 mg/mL; $S(q)_{eff}$ measured from 170 mg/mL protein solution was best fit using a hard sphere model. (h) $S(q)_{eff}$ measured from ammonium solution was best fit using a two-Yukawa model for all the studied protein concentrations. Error values in (a−d) correspond to 1 standard deviation.

protein concentrations, suggesting the presence of additional repulsive forces in sugar excipient conditions. The Stokes radius and protein volume fraction ϕ were used to calculate the theoretical $S(q)$; ϕ was calculated as $0.00132C$, where C was the protein concentration in mg/mL.[31] Results shown in Figure 1h suggest that the theoretical $S(q)$ calculated from the hard sphere model with valid input parameters can not be used to fit the experimental data measured at 50 mg/mL. The Hayter−Penfold model, which accounts for additional Coulomb repulsion, generated better fits for concentrated samples by assuming 12 charges per protein molecule. Therefore, appropriate fitting of $S(q)_{eff}$ confirmed that both excluded volume as well as the electrostatic repulsion between NISTmAb molecules contributed to the observed protein colloidal stability with sugar

DOI: 10.1021/acs.molpharmaceut.9b00687
Mol. Pharmaceutics 2019, 16, 4319−4338

excipients. This is in line with the proximity energy framework proposed by Laue that the presence of sugars such as sucrose and mannitol could lead to a decreased dielectric constant of solvent and, consequently, the increased charge−charge repulsion between adjacent antibody molecules.[69]

Nonspecific PPI play significant roles in the bulk rheological properties of antibody formulations, with both reversible attraction and electrostatic repulsion between protein molecules potentially leading to changes in η.[29,73] DLS/SLS and SAXS results implied that the PPI between NISTmAb molecules were altered in the presence of sugar excipients such that the molecules became more repulsive. Viscosity measurements were performed to examine changes in η. Experimental results showed that the addition of sugar excipients lead to an increase in η, and such a difference became more significant with increasing NISTmAb concentration (Figure 2a). Given the low effective charge of NISTmAb at pH 6, coupled with the suspected reduction in excluded volume, these results suggest that attractive dipole interactions may be controlling the increase in viscosity upon sugar addition at higher sample concentrations. Among the four sugars, disaccharides seemed to increase the value of η more significantly than the monosaccharide and sugar alcohol. With a protein concentration of 170 mg/mL, η values were around 25 cP for samples in sucrose and trehalose solutions, and glucose and mannitol solutions had similar η values of 21 cP. Similar results were reported by He that the disaccharides had more significant impacts on η than monosaccharides.[74]

Amino Acids as Excipients. Arginine, alanine, glycine, and proline were chosen to study the effects of commonly used amino acid excipients on the physical stability and solution viscosity of NISTmAb formulations. Results presented in Figure 3a show that the value of T_{onset} remained unchanged with the addition of arginine, whereas the presence of alanine, glycine, and proline led to increased T_{onset} values. Such changes in T_{onset} implied that the NISTmAb molecules were thermally stabilized by alanine, glycine, and proline, whereas arginine did not have any stabilizing effect on NISTmAb under the studied conditions. The R_g and R_H measured from NISTmAb are shown in Figure 3b; both values did not change much in alanine, glycine, and proline excipient conditions. Slight increases in both R_g and R_H values were observed with the presence of arginine, possibly because of direct interactions of NISTmAb with arginine molecules.[75,76] B_{22} and k_D values were estimated from dilute protein solutions and are represented in Figure 3c,d. Compared to the histidine control sample, the more positive B_{22} and k_D values implied the improved colloidal stability of NISTmAb possibly because of increased repulsive PPI. The ability of these amino acids on improving the thermal and colloidal stability of proteins has been reported.[77−79] However, different from alanine, glycine, and proline, the addition of arginine led to significant decreases in both B_{22} and k_D values, suggesting the more prominent attractive interactions between NISTmAb molecules; therefore, the colloidal stability was reduced in the arginine formulation condition.

Concentration-normalized scattering profiles obtained from NISTmAb concentration series in alanine formulation are shown in Figure 3e. $S(q)_{eff}$ derived from the scattering profiles deviated from unity with increasing protein concentrations, suggesting the presence of more significant PPI. This change in $S(q)_{eff}$ was also observed in other amino acid formulations. In order to better understand the nature of PPI that arose at higher protein concentrations, $S(q)_{eff}$ values were fitted using appropriate models. Because the values of $S(0)_{exp}$ were smaller than that of $S(0)_{HS}$ (Figure 3g), a Hayter−Penfold model was used to fit $S(q)_{eff}$ measured from alanine, glycine, and proline solutions. This is similar to the case of sugar excipients. $S(0)_{exp}$ calculated from arginine solution appeared to be less significant than $S(0)_{HS}$. Such a difference suggests the presence of attractive interactions to cancel out some of the repulsive forces, resulting in $S(0)_{exp}$ values closer to unity. Therefore, the two-Yukawa model, which accounts for both attractive and repulsive interactions, was used to fit $S(q)_{eff}$ measured from arginine solution (Figure 3h).

Finally, bulk solution viscosities were measured and compared with and without the addition of amino acid excipients (Figure 2b). All of the samples demonstrated increased η values with increasing protein concentrations. In the dilute concentration regime, η values of different samples were on the same order. As the solution became more concentrated, η values measured from arginine solution increased more rapidly than others; this is in line with the SAXS results that both repulsive and attractive interactions were present in arginine formulations. At 170 mg/mL, η values were measured to be 28.9 cP for arginine, 18.7 cP for proline, 16.3 cP for glycine, 15.8 cP for alanine formulation, and, finally, 12.2 cP for histidine control. Therefore, it can be concluded that the use of selected amino acid excipients can lead to an increased η of NISTmAb formulations.

Salts as Excipients. Anions and cations are ranked separately in the Hofmeister series by their abilities to stabilize protein through their interactions with water molecules.[80,81] Consequently, these ions are classified as the protein-stabilizing kosmotropes and the protein-destabilizing chaotropes. In this study, three anions, sulfate, chloride, and perchlorate, with distinct roles in the Hofmeister series were chosen so that the effects of kosmotropes and chaotropes on the physical stability and viscosity of NISTmAb formulations could be examined. In addition, ammonium ion was included to compare the cation with the anions. Anions examined in this study are ranked in the order of sulfate > chloride > perchlorate based on their propensity to stabilize proteins, whereas the ammonium ion is generally considered as a chaotrope due to its weak interaction with water molecules.[82] Figure 4a summarizes the effects of salts on the T_{onset} of NISTmAb in various salt solutions. As compared to the histidine control, slightly higher T_{onset} values were measured from sulfate and chloride solutions, whereas ammonium ions did not show any noticeable effect on T_{onset}. Different from other salt excipient conditions, a considerably low T_{onset} value was measured in perchlorate solution, implying protein molecules were thermally destabilized. Compared to the histidine control sample, both the R_g and R_H values of NISTmAb increased considerably in the presence of salts (Figure 4b); such a change in size could result from the more expanded conformation of NISTmAb or the increased attractive PPI between individual protein molecules. In the latter case, a decrease in B_{22} should be observed to correlate with the increased particle size. Figure 4c confirms that the addition of salt excipients led to decreased B_{22} values as a result of the attractive pairwise intermolecular interactions. Similarly, a reduction in k_D was observed for all of the examined salt solutions. The changes in both B_{22} and k_D values were indicative of the more significant attractive PPI as the result of charge screening.

SAXS experiments were performed to measure PPI directly at higher protein concentrations. SAXS profiles measured from NISTmAb at various concentrations overlapped with each other

DOI: 10.1021/acs.molpharmaceut.9b00687
Mol. Pharmaceutics 2019, 16, 4319−4338

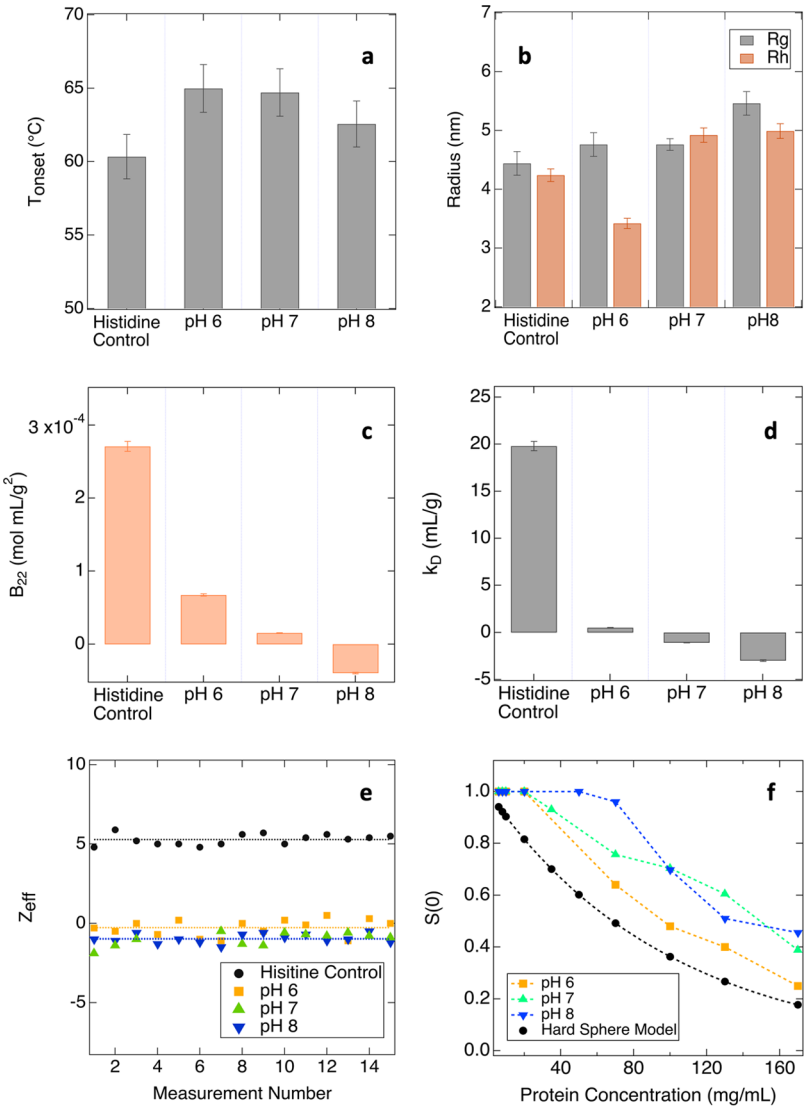

Figure 5. (a) Summary of T_{onset} of NISTmAb measured in different pH solutions. (b) R_g and R_H values of NISTmAb. (c,d) B_{22} and k_D calculated from NISTmAb in histidine and phosphate buffers. (e) Z_{eff} of NISTmAb measured in various buffer conditions; dotted lines represent the values of the average Z_{eff} based on 15 different measurements, and outliers are excluded from the calculation. (f) Changes in $S(0)_{exp}$ and $S(0)_{HS}$ values as a function of protein concentration; dotted lines were drawn to guide the eye. Error values in (a−d) correspond to 1 standard deviation.

at high q, suggesting the conformation of the individual NISTmAb molecule did not change with increasing concentration. On the contrary, scattering at lower q demonstrated concentration-dependent changes as the result of increased PPI (Figure 4e). From intermediate to high protein concentrations (between 40−130 mg/mL), $S(0)_{exp}$ measured from each salt excipient formulation appeared to be smaller than $S(0)_{HS}$ calculated from the hard sphere model, in which only repulsive interactions due to excluded volume effects were considered (Figure 4f). Therefore, $S(q)_{eff}$ values were best fitted with two-Yukawa model in this concentration range to account for both repulsive and attractive interactions. This is consistent with the observed reduction in k_D and B_{22} values. At higher protein concentrations, for example, 170 mg/mL, the contributions of various forces toward $S(q)_{eff}$ became different among various salt excipient conditions. Although $S(q)_{eff}$ could still be best described by the two-Yukawa model in the case of sulfate and ammonium salt solutions (Figure 4h), $S(q)_{eff}$ values measured from chloride and perchlorate solutions were best fitted using the hard sphere model (Figure 4g), implying that the attractive interactions between NISTmAb molecules were diminished under the studied conditions, and the excluded volume effect was the major contributor to the net PPI. The increased attractive interactions observed between NISTmAb molecules in salt solutions could be explained from the point of proximity energy framework theory that the activation energy barrier was lowered due to ion shielding; therefore, less energy was required for the monomers to form higher-order oligomers,[69] and as a result, the molecules became more attractive.

The effects of salts on the bulk solution viscosity are shown in Figure 2c. The value of η measured from histidine control was on a comparable level with the values measured from salt solutions until the protein concentration reached 80 mg/mL. Above this concentration, η values significantly increased as a result of salt modulation on the intermolecular interactions. At the highest examined protein concentration (170 mg/mL), NISTmAb solutions with sulfate and ammonium ions demonstrated the highest viscosity of 24.5 cP even though the attractive interactions were diminished, leaving excluded volume as the major contributor to the net repulsive PPI. With the presence of

DOI: 10.1021/acs.molpharmaceut.9b00687
Mol. Pharmaceutics 2019, 16, 4319−4338

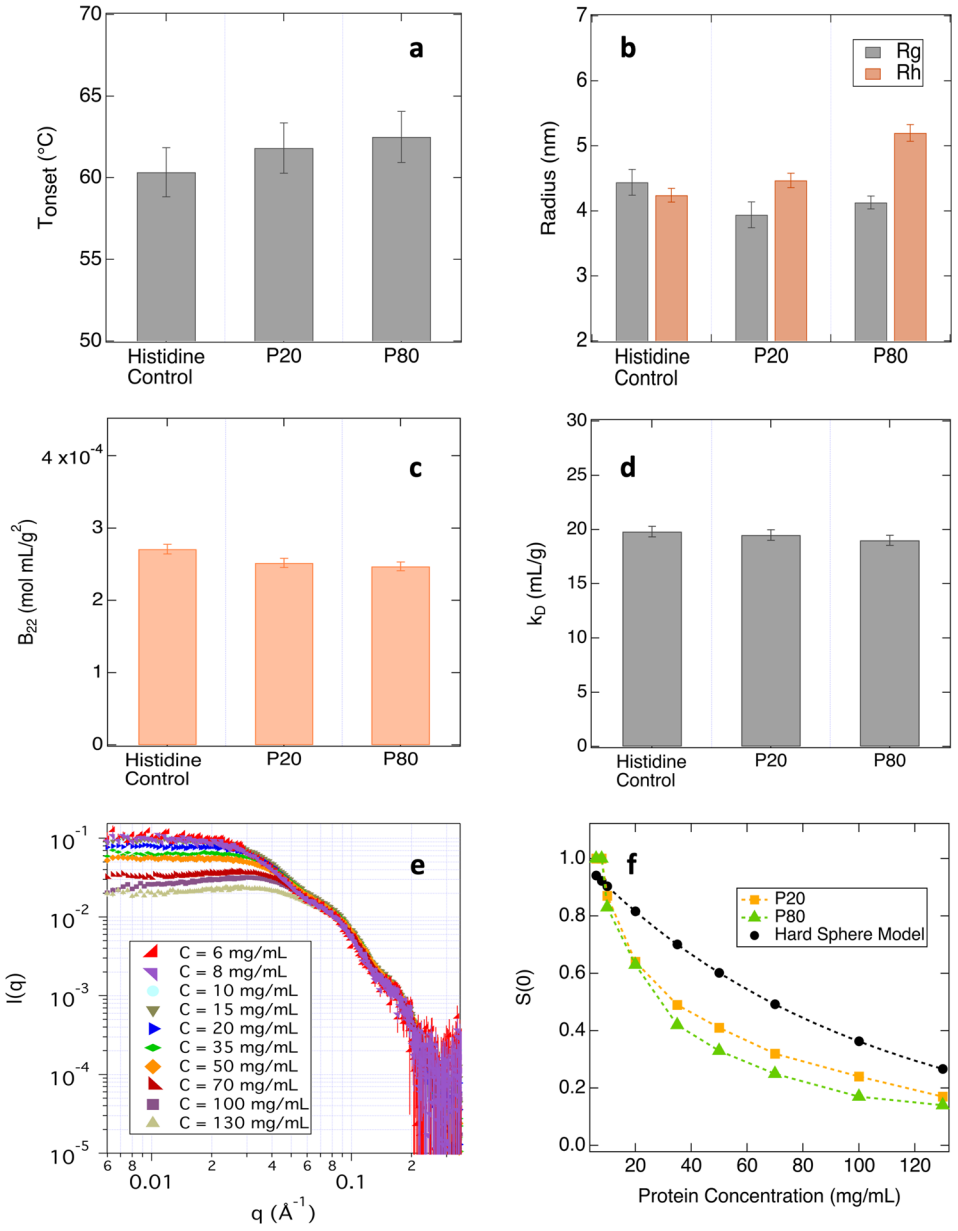

Figure 6. (a) Summary of T_{onset} measured from NISTmAb solutions with and without polysorbate excipients. (b) R_g and R_H of NISTmAb. (c,d) B_{22} and k_D values measured from histidine and polysorbate solutions. (e) Summary of SAXS profiles measured from P20 excipient formulations. (f) Changes in $S(0)_{exp}$ values as a function of protein concentration; dotted lines are drawn to guide the eye. Error values in (a–d) correspond to 1 standard deviation.

both attractive and repulsive interactions, the viscosities of chloride and perchlorate solutions were not as viscous as the other two salt solutions.

Effects of Solution pH. In order to study the effects of solution pH on the physical stability and viscosity of NISTmAb formulations, phosphate salts were used to prepare buffer solutions with three pH values of 6, 7, and 8. DSC results suggested that the thermal stability of NISTmAb was enhanced in phosphate buffer (Figure 5a). The R_g values of NISTmAb measured from phosphate buffer were greater than that measured from the histidine control. The observed R_H value was smallest at pH 6 and increased significantly as pH approached 7 (Figure 5b), whereas a further increase of solution pH to 8 led to negligible change in R_H. B_{22} and k_D values were calculated and are represented in Figure 5c,d. The effects of buffer species on PPI could be evaluated by comparing k_D and B_{22} values measured from histidine control with those measured from phosphate buffer both at pH 6. Much smaller k_D and B_{22} values were measured from phosphate buffer, suggesting NISTmAb molecules were less repulsive and, hence, less colloidally stable when using phosphate as buffering species. Comparing k_D and B_{22} values measured from phosphate buffers with different pH values, one can see that both values decreased with increasing solution pH. The negative k_D and B_{22} values measured from pH 8 solution suggested the PPI became net attractive, presumably because of the reduced surface charge of NISTmAb molecules. Figure 5e shows the effective surface charge Z_{eff} of NISTmAb measured from different buffer conditions. The absolute values of Z_{eff} significantly decreased when measured in phosphate buffer, suggesting NISTmAb molecules were less stable in such buffer conditions because of reduced electrostatic repulsions.

DOI: 10.1021/acs.molpharmaceut.9b00687
Mol. Pharmaceutics 2019, 16, 4319–4338

Figure 5f shows that $S(0)_{exp}$ values became less than 1 with increasing protein concentration, suggesting the more significant PPI between NISTmAb molecules in concentrated solutions. Moreover, the $S(0)_{exp}$ values measured from all three pH conditions were greater than the values of $S(0)_{HS}$, suggesting attractive interactions were present. This is in line with the observed changes in both k_D and B_{22} values measured from dilute protein solutions. Viscosity values measured from protein formulations prepared in 67 mM phosphate buffer were greater than those of formulations prepared in 25 mM histidine buffer. Among three phosphate buffers, the highest η was measured from pH 6 when the protein concentration was less than 130 mg/mL. Beyond 130 mg/mL, the solution viscosity was ranked in the order of pH 8, 7, and 6, with pH 8 buffer being the most viscous (Figure 2d).

Surfactants as Excipients. Polysorbates are a class of amphiphilic, nonionic surfactants composed of fatty acid esters of polyoxyethylene sorbitan. Among other polysorbates, polysorbate 20 and 80 are widely used in therapeutic protein formulations to prevent protein aggregation and adsorption onto the interfaces.[11] Therefore, the effects of polysorbate 20 and 80 (P20 and P80, respectively) on the physical stability and viscosity of NISTmAb formulations were examined (Figure 6). The use of polysorbates increased the T_{onset} of NISTmAb by ~2 °C as compared to the histidine control, suggesting NISTmAb molecules were more thermally stable in P20 and P80 solutions. Comparable R_g and R_H values were measured from NISTmAb with and without polysorbate excipients, confirming the stabilizing effects of polysorbates on protein conformation. The values of k_D and B_{22} were positive and decreased only slightly as compared to those of the histidine control sample, suggesting the net PPI were repulsive, and NISTmAb molecules were colloidally stable in polysorbate solutions.

SAXS results collected from P20 solution are shown in Figure 7e. $I(q)$ was reduced with increasing protein concentration at low q, suggesting the enhanced net repulsive PPI in a more crowded environment. Results shown in Figure 7f showed that $S(0)_{exp}$ values measured for polysorbate solutions were less than $S(0)_{HS}$ values, suggesting the presence of additional repulsive PPI apart from the excluded volume effect. The $S(q)_{eff}$ values measured from both P20 and P80 solutions were fitted using a Hayter–Penfold model by assuming eight charges per NISTmAb molecule. Finally, viscosity measurements suggested that both P20 and P80 did not have a significant impact on the measured η values when the protein concentration was less than 130 mg/mL. Above this concentration, the solution viscosity increased considerably with the presence of polysorbate excipients as compared to the histidine control sample (Figure 2e).

DISCUSSION

Excipients are an important component in therapeutic protein formulations. There are approximately 1000 excipients coming from 40 different functional categories used in marketed pharmaceutical products.[83] Excipients can have more than one function when included in a particular formulation. For example, they can act as protein stabilizers, diluents/fillers, and preservatives or to simply provide physiological osmolality.[13,84] When it comes to excipient selection, careful considerations must be given to the manufacturing process, the degradation mechanism of the protein/excipient, and, most importantly, the effects of each class of excipients on the physical and chemical stability of the protein therapeutics. Therefore, one of the objectives of this study is to characterize the physical stability of a model monoclonal antibody with the presence of commonly used excipients varying from sugar, amino acid, salt, pH, and surfactant. Different from other studies where the stability of proteins is examined as a function of excipient concentration, in this study, the physical stability of proteins was examined as a function of protein concentration at a fixed excipient concentration that is commonly used in antibody formulations.

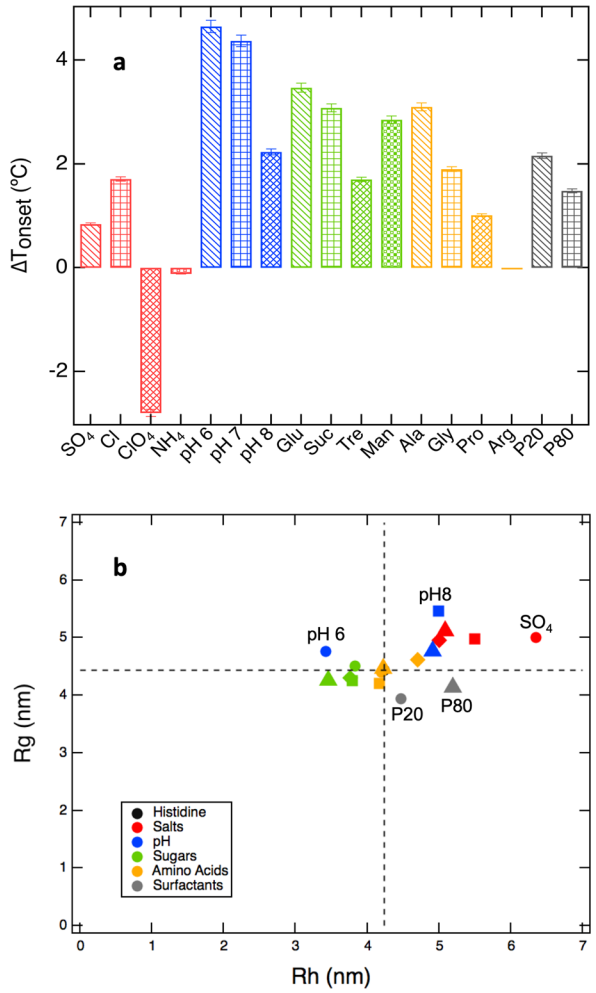

Figure 7. (a) Effects of excipients on the T_{onset} of NISTmAb in various formulation conditions. T_{onset} measured from histidine buffer was used as a reference for the calculation of ΔT_{onset} values: a positive ΔT_{onset} value is indicative of the increased T_{onset} value compared to that measured from a histidine reference and vice versa. Error bars represent 1 standard deviation. (b) Summary of R_H and R_g values measured from different excipient conditions. Dotted lines represent R_H and R_g values measured from 25 mM histidine buffer for better comparison.

Effects on Conformational Stability. NISTmAb prepared in 25 mM histidine buffer at pH 6 was considered as the control/reference for studying the excipient effects. The conformational stability of NISTmAb in various excipient formulations was assessed from two aspects: (1) the thermal stability of proteins, which was reflected by the melting temperature T_{onset}, and (2) the average size of proteins given by R_H and R_g, which provided information on the folding state of the protein. Excipient-induced changes in T_{onset} are summarized in Figure 7a, where the results show that improved protein thermal stability was achieved by using pH, sugar, and surfactant excipients. In the case of amino acids, alanine, glycine, and proline all lead to an

DOI: 10.1021/acs.molpharmaceut.9b00687
Mol. Pharmaceutics 2019, 16, 4319−4338

increased T_{onset}, whereas a negligible change in T_{onset} was measured from arginine solution. This result is consistent with a previous study that concluded that arginine does not stabilize proteins against heat treatment;[85] rather, it is used to prevent protein aggregation. Effects of salts on T_{onset} can be divided into two categories: kosmotropes like sulfate and chloride ions stabilized protein against thermal denaturation, whereas chaotropes including perchlorate and ammonium ions destabilized protein against thermal denaturation.

The conformational stability of NISTmAb was also examined by measuring both R_H and R_g of the protein in various excipient formulations (Figure 7b). In general, both sugar and amino acid excipients did not lead to significant changes in the apparent sizes of NISTmAb. The presence of polysorbates resulted in a slight decrease in R_g and an increase in R_H, whereas the use of salts led to increases in both values. An increase in R_g was observed when substituting histidine with phosphate buffer, a decrease in R_H was observed in pH 6 phosphate buffer, and increased R_H values were observed in pH 7 and 8 buffer conditions. We have previously reported that the NISTmAb can adopt a wide range of R_g values from 39 to 55 Å when taking the flexibility of hinge region into account. In this study, the measured R_g values from all the examined excipient conditions were all within this range.[49] Although it is not anticipated that the association of excipient molecules to the protein surface can lead to significant changes in the R_g values of all possible NISTmAb structures, it is expected that the solution properties of the excipient formulation can shift the average value of R_g and, hence, R_H to more extended or compact states depending on the complex dynamic interactions with excipients and the protein surface.

Effects on Colloidal Stability. Nonspecific PPI are generally considered as a major determinant for protein colloidal stability. As a result, PPI are often characterized and used as a predictive tool for studying the long-term stability of proteins in solution.[15,86] The net PPI could be either attractive or repulsive. Repulsive PPI imply protein molecules are spatially separated due to repulsive forces, hence colloidally stable, whereas attractive PPI suggest proteins are prone to self-associate; thus, they are considered as less colloidally stable. Therefore, conditions under which attractive PPI are dominated should be avoided. In this study, the colloidal stability of NISTmAb in various excipient conditions was examined for a wide range of protein concentrations. Two sets of experimental parameters were measured from dilute (k_D and B_{22} from DLS/SLS) and concentrated ($S(q)_{eff}$ from SAXS) protein solutions in order to better characterize the nature of PPI. Also, the validity of DLS/SLS for studying PPI in concentrated protein solutions was evaluated by comparing the two data sets.

Estimated from sufficiently dilute protein solutions, k_D and B_{22} are measures of the nonideal solution behavior due to the presence of nonspecific PPI. Although both parameters describe the property of dilute protein solutions, they are widely used in the pharmaceutical industry for predicting protein colloidal stability at much higher concentrations. The changes in both k_D and B_{22} with the presence of various excipients are summarized in Figure 8. Although B_{22} values measured from NISTmAb in sugar solutions were reduced, the k_D values were either unchanged or became even more positive as compared to that measured from histidine control, suggesting the increased contribution from the solvent-mediated hydrodynamic interactions.[28,70] In the case of amino acid excipients, the presence of alanine, proline, and glycine led to increased k_D and B_{22} values,

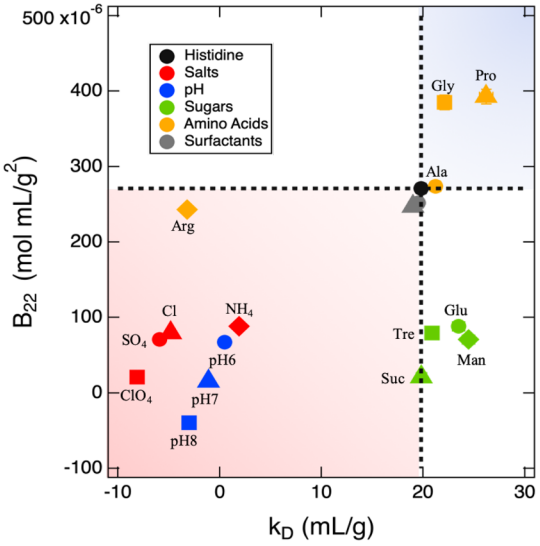

Figure 8. Summary of k_D and B_{22} values measured from various excipient conditions. Dotted lines represent k_D and B_{22} values measured from 25 mM histidine buffer as a reference. Errors represent 1 standard deviation.

suggesting NISTmAb molecules were more colloidally stable in these excipient formulations. Although arginine has been widely used in protein formulations to prevent protein aggregation, changes in k_D and B_{22} values suggested the PPI became more attractive with the presence of arginine. Together with the DSC result, it is shown that neither the thermal nor the colloidal stability of NISTmAb was improved in 200 mM arginine solution. Among different excipient categories, pH and salts significantly reduced the values of both k_D and B_{22} as compared to those measured from histidine control, suggesting the PPI became more attractive under these excipient conditions. Interestingly, there was a negative linear relationship among the solution pH and k_D and B_{22} values, suggesting the higher the pH, the more attractive the PPI. The isoelectric point (pI) of NISTmAb is pH 9.2;[87] therefore, the net charge of NISTmAb decreases with increasing solution pH from 6 to 8. The observed increase in attractive PPI could result from the reduced long-ranged electrostatic repulsion between individual protein molecules. Similarly, the decrease in k_D and B_{22} values with the presence of salt excipients could be the result of the reduced net charge of proteins resulting from Debye screening.[31] Polysorbates did not seem to have any significant impact on k_D and B_{22} values, implying NISTmAb molecules were similarly colloidally stable in polysorbate solutions as they were in histidine buffer.

Different from k_D and B_{22}, $S(q)_{eff}$ values were measured directly from concentrated protein solutions; thus, more straightforward characterization of PPI at higher protein concentrations was allowed. For all of the examined excipient conditions, the $S(0)_{exp}$ values became less than unity with increasing protein concentrations. Such changes suggested that the nonspecific PPI became more significant at higher protein concentrations and that the net PPI were repulsive. Therefore, NISTmAb molecules were, in general, colloidally stable in all of the examined excipient formulations. Previous research reported the cutoff value of k_D between net attractive and net repulsive interactions to be ∼−8 mL/g for antibody formulations;[88−91] therefore, we can conclude from such a k_D value that the PPI of NISTmAb were of net repulsive nature in all of the examined

DOI: 10.1021/acs.molpharmaceut.9b00687
Mol. Pharmaceutics 2019, 16, 4319−4338

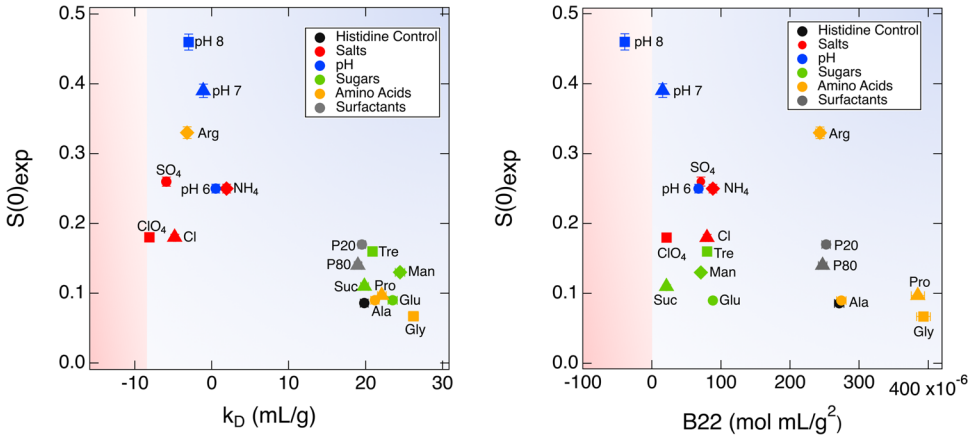

Figure 9. Summary of $S(0)_{exp}$ against k_D (left) and B_{22} (right) measured from all of the examined excipient conditions. Backgrounds are highlighted to separate regions where $S(0)_{exp}$ is correlated with k_D and B_{22} values for net attractive or repulsive PPI. Data sets are colored among different excipient categories. Error bars correspond to 1 standard deviation. $S(0)_{exp}$ values were measured from highest examined protein concentrations (from 130 to 170 mg/mL).

excipient conditions. This is in close agreement with the conclusion that we made from $S(0)_{exp}$ results (Figure 9). In the case of B_{22}, it is generally regarded that a positive B_{22} value is a sign of net repulsive interactions; therefore, a $S(0)_{exp}$ value less than 1 should correlate with a positive B_{22} value in the case of net repulsive interactions. From Figure 9, we can see that the $S(0)_{exp}$ correlates well with B_{22} for most of the excipient conditions except pH 8 phosphate buffer. Therefore, on the basis of the presented results, it is fair to conclude that the use of DLS/SLS is valid for predicting the colloidal stability of NISTmAb in concentrated solutions.

Although the net PPI were repulsive as evident by the $S(q)_{eff}$, further analysis of $S(q)_{eff}$ allowed the dissection of net PPI into various attractive and repulsive forces, allowing better prediction of protein colloidal stability and more efficient formulation design. It is believed that in highly concentrated protein solutions, the hydrodynamic forces resulting from excluded volume are the most significant contributor to PPI;[15,22] therefore, $S(0)_{exp}$ values measured from each excipient condition were compared to $S(0)_{HS}$ derived from hard sphere model. Results showed that the values of $S(0)_{exp}$ became more different from $S(0)_{HS}$ with increasing protein concentration, suggesting the more significant roles played by other forces apart from excluded volume effect. If $S(0)_{exp}$ is greater than $S(0)_{HS}$, then the PPI are more attractive as compared to that of the hard sphere model and vice versa. Therefore, by comparing the two values, it can be concluded that NISTmAb molecules were less colloidally stable in salt and pH (close to pI) excipient conditions, whereas NISTmAb molecules were further stabilized by Coulombic repulsions with the presence of sugars, most amino acids, and polysorbates. A summary of $S(0)_{exp}/S(0)_{HS}$ values (Figure S1) and fitting parameters for the Hayter–Penfold model (Table S1) are presented in the Supporting Information.

Effects on Bulk Solution Viscosity. Different mAbs can demonstrate vastly different viscosity properties in solution. For example, the measured η values for 150 mg/mL mAb solutions could be in the range between a few cP to hundreds of cP; therefore, the high viscosity of concentrated mAb solution can represent a challenge in the formulation and development of mAb therapeutics.[73,92,93] Unlike some mAbs that demonstrate a significant increase in η values with increasing concentration, the concentration dependence of NISTmAb is comparably lower. A positive relationship between NISTmAb concentration and the η was observed from all of the examined excipient formulations. For highly concentrated protein solutions (170 mg/mL), the use of excipients resulted in a more viscous solution as compared to the histidine control (Figure 2). The greater η values measured from concentrated protein solutions were related to the enhanced PPI and possibly, the presence of transient protein clusters as seen for other mAbs.[73,94] k_D and B_{22} values are traditionally used to predict the bulk solution viscosities of concentrated antibody formulations, because they provide information on the intermolecular interactions. Therefore, the predicted results returned from k_D and B_{22} values were compared with experimentally determined η values (Figure 10). If we consider excipient-mediated PPI as the major contributor to η, then it is widely accepted that an increase in the attractive PPI, which is reflected by a decrease in k_D and B_{22} values as compared to the histidine control, is indicative of increased η, whereas an increase in repulsive PPI is indicative of reduced η.[14,22] Figure 10 summarizes the correlations among k_D, B_{22}, and η for each excipient condition; shaded areas highlighted samples from which the changes in k_D and B_{22} demonstrated the above-mentioned correlations with η. From the correlation plot between k_D and η, it can be seen that although a large number of samples resided within the shaded areas, exceptions were observed for samples with amino acid and sugar excipients (except arginine), suggesting the disagreements between the predicted and measured viscosity results for these excipient conditions. Compared to k_D, better correlations were found between B_{22} and η values; in this case, samples with sugar, salt, pH, and surfactant excipients all demonstrated decreased B_{22} values with a concomitant increase in η. The only two samples that did not follow the predicted correlation between B_{22} and η were samples with glycine and proline excipients. In the case of arginine, a decrease in B_{22} was measured concomitantly with an increased η value. These changes were in line with the commonly accepted correlation that increased PPI (reflected by a decrease in B_{22}) can lead to increased solution viscosity.[95] Although as compared to the histidine control sample, a small decrease in B_{22} was correlated with a rather significant increase in η; thus, this observation suggests that the increase in solution viscosity was not only attributed to increased attractive PPI. Other factors, such as the formation of transient protein clusters, could also lead to increased viscosity.[96] Directly measured from

DOI: 10.1021/acs.molpharmaceut.9b00687
Mol. Pharmaceutics 2019, 16, 4319–4338

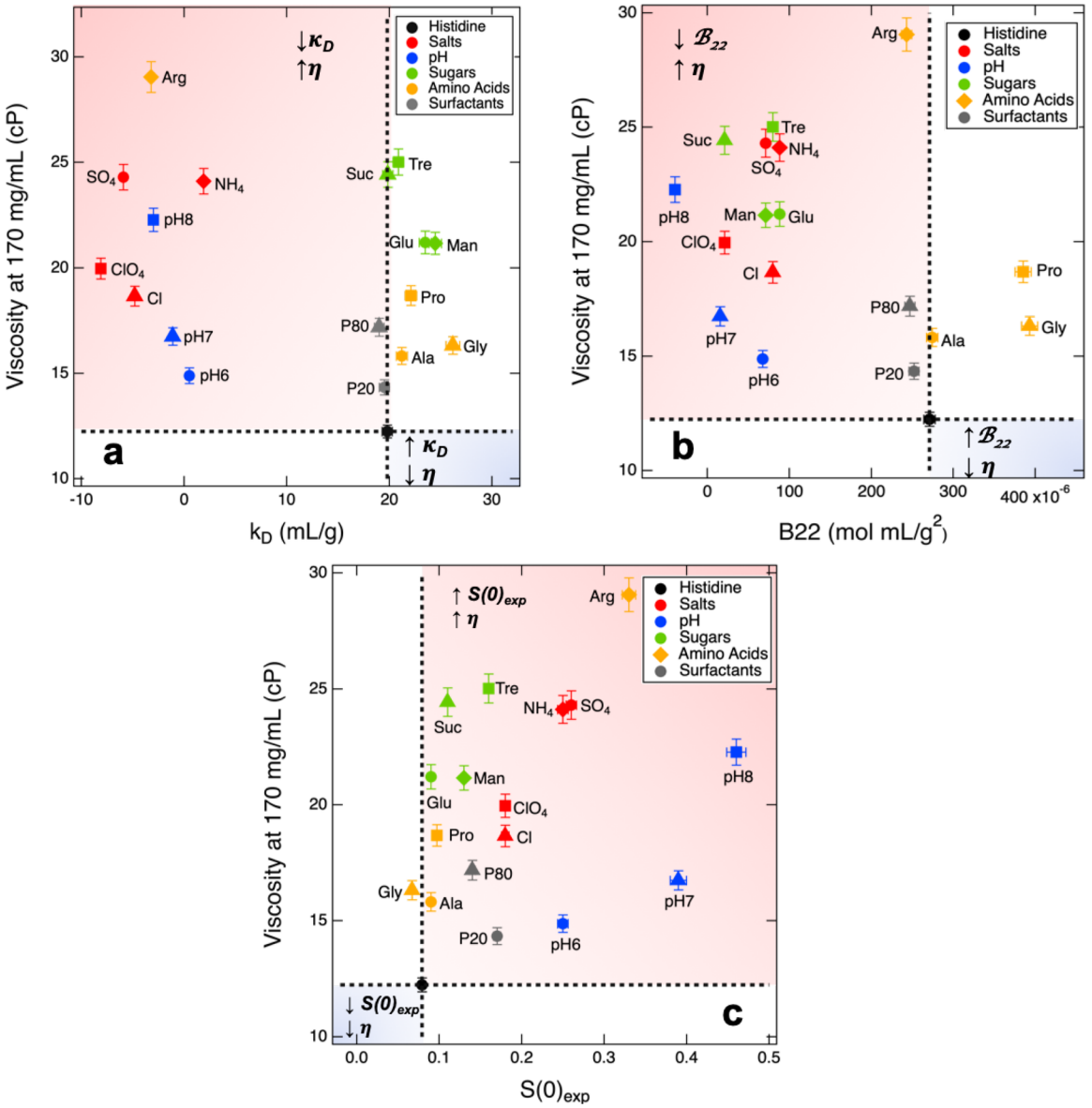

Figure 10. Correlation between η values measured at 170 mg/mL protein concentration with k_D (a), B_{22} (b), and $S(0)_{exp}$ (c) values. The red shaded area highlights samples from which a decrease in k_D/B_{22} or an increase in $S(0)_{exp}$ is correlated with an increase in η. The blue shaded area highlights samples from which an increase in k_D/B_{22} or a decrease in $S(0)_{exp}$ is correlated with a decrease in η. The dotted lines highlight the results of NISTmAb in 25 mM histidine buffer as a reference. Data sets are colored among different excipient categories, and error bars represent 1 standard deviation.

concentrated solutions, $S(q)_{eff}$ provides valuable information on PPI that are present in crowded environments; therefore, the correlation between $S(0)_{exp}$ and η values was also examined and is represented in Figure 10. As compared to histidine control, it is anticipated that an increased $S(0)_{exp}$ value measured in the presence of excipient is indicative of more attractive PPI of NISTmAb; hence, larger η values should be measured. Results show that the increase in $S(0)_{exp}$ was correlated with increased η value for nearly all of the examined excipient conditions except glycine, where a slight decrease in $S(0)_{exp}$ was observed. Therefore, on the basis of the comparison between the predicted and measured results on bulk solution viscosity, one can conclude that $S(0)_{exp}$ and B_{22} are better predictors than k_D for the viscosities of concentrated NISTmAb formulations. The disagreements found between the predicted and measured viscosity results imply other factors apart from the PPI contribute to the bulk rheological properties of concentrated protein solutions. Therefore, careful examination by multiple techniques is recommended for better formulation screening.

Selection of Excipients for Improved Physical Stability. Proteins aggregate through different pathways. Aggregation could result from the association of either the unfolded or native protein molecules;[97] therefore, excipients should be selected so that not only the unfolding but also the self-association of protein molecules are minimized. The effects of excipients on the physical stability of NISTmAb were assessed by a variety of biophysical characterization techniques as either the changes in T_m (conformational stability) or the changes in net PPI (colloidal stability). The stabilizing effects of various excipients have been studied for many proteins.[12,16,18,38,68,98−101] Although efforts have been made in seeking a general mechanism through which proteins are stabilized by each category, excipients seem to act differently on different proteins.[12,16,18,38,68,98−101] Moreover, the ability of excipients to improve the conformational

DOI: 10.1021/acs.molpharmaceut.9b00687
Mol. Pharmaceutics 2019, 16, 4319−4338

stability of proteins does not always correlate with their ability to improve the colloidal stability, as these are resulted from different intra- or intermolecular forces. For example, the ability of sugars to protect proteins from thermal unfolding is known.[67,68,102] The current understanding of the stabilizing mechanism is that sugar molecules are excluded from the protein surface because of their preferential interactions with each other and surrounding water molecules. As a result, the surface tension of protein molecules elevates, increasing the energetic penalty for unfolding. That is, greater energy is required to unfold proteins in the presence of sugars; this, in turn, leads to the improved thermal stability of proteins.[67] Although sugar molecules can stabilize proteins against thermal unfolding, their impacts on the colloidal stability of proteins are pH-, buffer-ionic-strength-, protein-, and sugar-dependent.[16,18,23] In the case of amino acids, although most of them are generally considered as both conformational and colloidal stabilizers for protein molecules,[103,104] the role of arginine is more complicated. Arginine could have either positive or negative impacts on the physical stability of proteins depending on protein types and anions associated with the arginine salt.[18,85,105] Therefore, the impact of various excipients on both the conformational and colloidal stabilities of desired protein therapeutics should be carefully considered to ensure the balanced selection of excipient formulations.

CONCLUSIONS

The effects of commonly used excipients on the physical stability and viscosity of NISTmAb formulations are evaluated in this study. Collectively, the experimental results show that NISTmAb molecules are both conformationally and colloidally stable in all of the examined excipient conditions. Although the net PPI are repulsive, a detailed analysis of $S(q)_{eff}$ reveals that the intermolecular interactions become more attractive in salt, pH, and arginine excipient formulations (i.e., ionic excipients). The uses of k_D, B_{22} (measured from dilute samples), and $S(0)_{exp}$ (measured from concentrated sample) for studying the colloidal stability of NISTmAb in concentrated formulations were compared, and a close agreement was found between the two sets of parameters. NISTmAb formulations demonstrated a concentration- and excipient-dependent increase in bulk solution viscosities. The comparison between predicted and experimental results on solution viscosity suggest that $S(0)_{exp}$ and B_{22} are better predictors for η than k_D for concentrated NISTmAb formulations. However, the reliability of prediction is limited to certain excipient conditions, as not all samples follow the general trend. It is anticipated that other factors besides PPI contribute significantly toward the elevated solution viscosity at higher protein concentrations.

ASSOCIATED CONTENT

Supporting Information

The Supporting Information is available free of charge on the ACS Publications website at DOI: 10.1021/acs.molpharmaceut.9b00687.

Summary of $S(0)_{exp}/S(0)_{HS}$ values as well as the fitting parameters of Hayter–Penfold model for various excipient conditions (PDF)

AUTHOR INFORMATION

Corresponding Author

*E-mail: joseph.curtis@nist.gov.

ORCID

Amy Yuanyuan Xu: 0000-0002-4071-1750

Present Address

§Drug Product Development US, GSK Vaccines, 14200 Shady Grove Road, Rockville, Maryland 20850, United States. (M.M.C.)

Notes

The authors declare no competing financial interest.

ACKNOWLEDGMENTS

The authors thank Dr. Alexander Grishaev for the assistance with SAXS measurements at the Institute of Bioscience and Biotechnology Research, University of Maryland. The NIST-mAb reference material is generously provided by Dr. John E. Schiel from Bioanalytical Science Group, NIST. A.Y.X. and M.M.C. acknowledge financial support from the NIST biomanufacturing initiative. This work used CCP-SAS software developed through a joint EPSRC (EP/K039121/1) and NSF (CHE-1265821) grant.

REFERENCES

(1) Garidel, P.; Hegyi, M.; Bassarab, S.; Weichel, M. A rapid, sensitive and economical assessment of monoclonal antibody conformational stability by intrinsic tryptophan fluorescence spectroscopy. *Biotechnol. J.* **2008**, *3*, 1201–11.

(2) Razinkov, V. I.; Treuheit, M. J.; Becker, G. W. Accelerated formulation development of monoclonal antibodies (mAbs) and mAb-based modalities: review of methods and tools. *J. Biomol. Screening* **2015**, *20*, 468–83.

(3) Garidel, P.; Kuhn, A. B.; Schäfer, L. V.; Karow-Zwick, A. R.; Blech, M. High-concentration protein formulations: How high is high? *Eur. J. Pharm. Biopharm.* **2017**, *119*, 353–360.

(4) Inoue, N.; Takai, E.; Arakawa, T.; Shiraki, K. Specific decrease in solution viscosity of antibodies by arginine for therapeutic formulations. *Mol. Pharmaceutics* **2014**, *11*, 1889–96.

(5) Shire, S. J.; Shahrokh, Z.; Liu, J. Challenges in the development of high protein concentration formulations. *J. Pharm. Sci.* **2004**, *93*, 1390–402.

(6) Yanase, K.; Arai, R.; Sato, T. Intermolecular interactions and molecular dynamics in bovine serum albumin solutions studied by small angle X-ray scattering and dielectric relaxation spectroscopy. *J. Mol. Liq.* **2014**, *200*, 59–66.

(7) Braun, M. K.; Grimaldo, M.; Roosen-Runge, F.; Hoffmann, I.; Czakkel, O.; Sztucki, M.; Zhang, F.; Schreiber, F.; Seydel, T. Crowding-controlled cluster size in concentrated aqueous protein solutions: structure, self- and collective diffusion. *J. Phys. Chem. Lett.* **2017**, *8*, 2590–2596.

(8) Liu, Y.; Porcar, L.; Chen, J.; Chen, W.-R.; Falus, P.; Faraone, A.; Fratini, E.; Hong, K.; Baglioni, P. Lysozyme protein solution with an intermediate range order structure. *J. Phys. Chem. B* **2011**, *115*, 7238–7247.

(9) Wu, H.; Truncali, K.; Ritchie, J.; Kroe-Barrett, R.; Singh, S.; Robinson, A. S.; Roberts, C. J. Weak protein interactions and pH- and temperature-dependent aggregation of human Fc1. *MAbs* **2015**, *7*, 1072–83.

(10) Roberts, C. J. Therapeutic protein aggregation: mechanisms, design, and control. *Trends Biotechnol.* **2014**, *32*, 372–80.

(11) Kamerzell, T. J.; Esfandiary, R.; Joshi, S. B.; Middaugh, C. R.; Volkin, D. B. Protein-excipient interactions: mechanisms and biophysical characterization applied to protein formulation development. *Adv. Drug Delivery Rev.* **2011**, *63*, 1118–59.

(12) Falconer, R. J.; Chan, C.; Hughes, K.; Munro, T. P. Stabilization of a monoclonal antibody during purification and formulation by addition of basic amino acid excipients. *J. Chem. Technol. Biotechnol.* **2011**, *86*, 942–948.

DOI: 10.1021/acs.molpharmaceut.9b00687
Mol. Pharmaceutics 2019, 16, 4319–4338

(13) Ohtake, S.; Kita, Y.; Arakawa, T. Interactions of formulation excipients with proteins in solution and in the dried state. *Adv. Drug Delivery Rev.* **2011**, *63*, 1053−73.
(14) Koo, O., Ed. *Pharmaceutical excipients: properties, functionality, and applications in research and industry*; Wiley, 2016.
(15) Sorret, L. L.; DeWinter, M. A.; Schwartz, D. K.; Randolph, T. W. Challenges in predicting protein-protein interactions from measurements of molecular diffusivity. *Biophys. J.* **2016**, *111*, 1831−1842.
(16) James, S.; McManus, J. J. Thermal and solution stability of lysozyme in the presence of sucrose, glucose, and trehalose. *J. Phys. Chem. B* **2012**, *116*, 10182−8.
(17) Kerwin, B. A. Polysorbates 20 and 80 used in the formulation of protein biotherapeutics: structure and degradation pathways. *J. Pharm. Sci.* **2008**, *97*, 2924−35.
(18) Sudrik, C.; Cloutier, T.; Pham, P.; Samra, H. S.; Trout, B. L. Preferential interactions of trehalose, L-arginine.HCl and sodium chloride with therapeutically relevant IgG1 monoclonal antibodies. *MAbs* **2017**, *9*, 1155−1168.
(19) Garidel, P.; Blume, A.; Wagner, M. Prediction of colloidal stability of high concentration protein formulations. *Pharm. Dev. Technol.* **2015**, *20*, 367−74.
(20) Chaudhuri, R.; Cheng, Y.; Middaugh, C. R.; Volkin, D. B. High-throughput biophysical analysis of protein therapeutics to examine interrelationships between aggregate formation and conformational stability. *AAPS J.* **2014**, *16*, 48−64.
(21) Hofmann, M.; Winzer, M.; Weber, C.; Gieseler, H. Prediction of protein aggregation in high concentration protein solutions utilizing protein-protein interactions determined by low volume static light scattering. *J. Pharm. Sci.* **2016**, *105*, 1819−1828.
(22) Tomar, D. S.; Kumar, S.; Singh, S. K.; Goswami, S.; Li, L. Molecular basis of high viscosity in concentrated antibody solutions: Strategies for high concentration drug product development. *MAbs* **2016**, *8*, 216−28.
(23) Wen, L.; Zheng, X.; Wang, X.; Lan, H.; Yin, Z. Bilateral effects of excipients on protein stability: preferential interaction type of excipient and surface aromatic hydrophobicity of protein. *Pharm. Res.* **2017**, *34*, 1378−1390.
(24) Saluja, A.; Fesinmeyer, R. M.; Hogan, S.; Brems, D. N.; Gokarn, Y. R. Diffusion and sedimentation interaction parameters for measuring the second virial coefficient and their utility as predictors of protein aggregation. *Biophys. J.* **2010**, *99*, 2657−65.
(25) Neergaard, M. S.; Kalonia, D. S.; Parshad, H.; Nielsen, A. D.; Møller, E. H.; van de Weert, M. Viscosity of high concentration protein formulations of monoclonal antibodies of the IgG1 and IgG4 subclass - prediction of viscosity through protein-protein interaction measurements. *Eur. J. Pharm. Sci.* **2013**, *49*, 400−10.
(26) Hofmann, M.; Gieseler, H. Predictive screening tools used in high-concentration protein formulation development. *J. Pharm. Sci.* **2018**, *107*, 772−777.
(27) Woldeyes, M. A.; Qi, W.; Razinkov, V. I.; Furst, E. M.; Roberts, C. J. How well do low- and high-concentration protein interactions predict solution viscosities of monoclonal antibodies? *J. Pharm. Sci.* **2019**, *108*, 142−154.
(28) Blanco, M. A.; Perevozchikova, T.; Martorana, V.; Manno, M.; Roberts, C. J. Protein-protein interactions in dilute to concentrated solutions: a-chymotrypsinogen in acidic conditions. *J. Phys. Chem. B* **2014**, *118*, 5817−31.
(29) Saluja, A.; Kalonia, D. S. Nature and consequences of protein-protein interactions in high protein concentration solutions. *Int. J. Pharm.* **2008**, *358*, 1−15.
(30) Castellanos, M. M.; Howell, S. C.; Gallagher, D. T.; Curtis, J. E. Characterization of the NISTmAb Reference Material using small-angle scattering and molecular simulation: Part I: Dilute protein solutions. *Anal. Bioanal. Chem.* **2018**, *410*, 2141−2159.
(31) Castellanos, M. M.; Mattison, K.; Krueger, S.; Curtis, J. E. Characterization of the NISTmAb Reference Material using small-angle scattering and molecular simulation: Part II: Concentrated protein solutions. *Anal. Bioanal. Chem.* **2018**, *410*, 2161−2171.
(32) Kaieda, S.; Lund, M.; Plivelic, T. S.; Halle, B. Weak self-interactions of globular proteins studied by small-angle X-ray scattering and structure-based modeling. *J. Phys. Chem. B* **2014**, *118*, 10111−9.
(33) Tian, X.; Langkilde, A. E.; Thorolfsson, M.; Rasmussen, H. B.; Vestergaard, B. Small-angle x-ray scattering screening complements conventional biophysical analysis: comparative structural and biophysical analysis of monoclonal antibodies IgG1, IgG2, and IgG4. *J. Pharm. Sci.* **2014**, *103*, 1701−10.
(34) Mosbæk, C. R.; Konarev, P. V.; Svergun, D. I.; Rischel, C.; Vestergaard, B. High concentration formulation studies of an IgG2 antibody using small angle X-ray scattering. *Pharm. Res.* **2012**, *29*, 2225−35.
(35) Dong, Q.; Liang, Y.; Yan, X.; Markey, S. P.; Mirokhin, Y. A.; Tchekhovskoi, D. V.; Bukhari, T. H.; Stein, S. E. The NISTmAb tryptic peptide spectral library for monoclonal antibody characterization. *MAbs* **2018**, *10*, 354.
(36) Schiel, J. E.; Turner, A.; Mouchahoir, T.; Yandrofski, K.; Telikepalli, S.; King, J.; DeRose, P.; Ripple, D.; Phinney, K. The NISTmAb Reference Material 8671 value assignment, homogeneity, and stability. *Anal. Bioanal. Chem.* **2018**, *410*, 2127−2139.
(37) Gokarn, Y. Biophysical Techniques for Characterizing the Higher Order Structure and Interactions of Monoclonal Antibodies. *State-of-the-Art and Emerging Technologies for Therapeutic Monoclonal Antibody Characterization Volume 2. Biopharmaceutical Characterization: The NISTmAb Case Study* **2015**, *1201*, 285−327.
(38) Mahler, H.-C.; Senner, F.; Maeder, K.; Mueller, R. Surface activity of a monoclonal antibody. *J. Pharm. Sci.* **2009**, *98*, 4525−4533.
(39) Singh, S. M.; Bandi, S.; Jones, D. N. M.; Mallela, K. M. G. Effect of polysorbate 20 and polysorbate 80 on the higher-order structure of a monoclonal antibody and its fab and fc fragments probed using 2D nuclear magnetic resonance spectroscopy. *J. Pharm. Sci.* **2017**, *106*, 3486−3498.
(40) Kaszuba, M.; McKnight, D.; Connah, M. T.; McNeil-Watson, F. K.; Nobbmann, U. Measuring sub nanometre sizes using dynamic light scattering. *J. Nanopart. Res.* **2008**, *10*, 823−829.
(41) HARDING, S. E.; JOHNSON, P. The concentration-dependence of macromolecular parameters. *Biochem. J.* **1985**, *231*, 543−547.
(42) Salgin, S.; Salgin, U.; Bahadir, S. Zeta potentials and isoelectric points of biomolecules: the effects of ion types and ionic strengths. *Int. J. Electrochem. Sci.* **2012**, *7*, 12404−12414.
(43) Kaszuba, M.; Corbett, J.; Watson, F. M.; Jones, A. High-concentration zeta potential measurements using light-scattering techniques. *Philos. Trans. R. Soc., A* **2010**, *368*, 4439−51.
(44) Nielsen, S. S.; Toft, K. N.; Snakenborg, D.; Jeppesen, M. G.; Jacobsen, J. K.; Vestergaard, B.; Kutter, J. P.; Arleth, L. BioXTAS RAW, a software program for high-throughput automated small-angle X-ray scattering data reduction and preliminary analysis. *J. Appl. Crystallogr.* **2009**, *42*, 959−964.
(45) Guinier, A. La diffraction des rayons X aux tres petits angles: applications a l'etude de phenomenes ultramicroscopiques. *Ann. Phys.* **1939**, *11*, 161−237.
(46) Gelamo, E. L.; Itri, R.; Tabak, M. Small angle x-ray scattering (SAXS) study of the extracellular Hemoglobin of Glossoscolex paulistus: effect of pH, iron oxidation state, and interaction with anionic SDS surfactant. *J. Biol. Chem.* **2004**, *279*, 33298−305.
(47) Castellanos, M. M.; McAuley, A.; Curtis, J. E. Investigating structure and dynamics of proteins in amorphous phases using neutron scattering. *Comput. Struct. Biotechnol. J.* **2017**, *15*, 117−130.
(48) Curtis, J. E.; Raghunandan, S.; Nanda, H.; Krueger, S. SASSIE: A program to study intrinsically disordered biological molecules and macromolecular ensembles using experimental scattering restraints. *Comput. Phys. Commun.* **2012**, *183*, 382−389.
(49) Castellanos, M. M.; Clark, N. J.; Watson, M. C.; Krueger, S.; McAuley, A.; Curtis, J. E. Role of molecular flexibility and colloidal descriptions of proteins in crowded environments from small-angle scattering. *J. Phys. Chem. B* **2016**, *120*, 12511−12518.
(50) Clark, N. J.; Zhang, H.; Krueger, S.; Lee, H. J.; Ketchem, R. R.; Kerwin, B.; Kanapuram, S. R.; Treuheit, M. J.; McAuley, A.; Curtis, J. E.

DOI: 10.1021/acs.molpharmaceut.9b00687
Mol. Pharmaceutics 2019, 16, 4319−4338

Small-angle neutron scattering study of a monoclonal antibody using free-energy constraints. *J. Phys. Chem. B* **2013**, *117*, 14029−14038.
(51) Heidorn, D. B.; Trewhella, J. Comparison of the crystal and solution structures of calmodulin and troponin C. *Biochemistry* **1988**, *27*, 909−15.
(52) Krueger, S.; Gorshkova, I.; Brown, J.; Hoskins, J.; McKenney, K. H.; Schwarz, F. P. Determination of the conformations of cAMP receptor protein and its T127L,S128A mutant with and without cAMP from small angle neutron scattering measurements. *J. Biol. Chem.* **1998**, *273*, 20001−6.
(53) Koch, M. H.; Vachette, P.; Svergun, D. I. Small-angle scattering: a view on the properties, structures and structural changes of biological macromolecules in solution. *Q. Rev. Biophys.* **2003**, *36*, 147−227.
(54) PERCUS, J. K.; YEVICK, G. J. Analysis of classical statistical mechanics by means of collective coordinates. *Phys. Rev.* **1958**, *110*, 1−13.
(55) HAYTER, J. B.; PENFOLD, J. An analytic structure factor for macroion solutions. *Mol. Phys.* **1981**, *42*, 109−118.
(56) Chen, S.-H.; Broccio, M.; Liu, Y.; Fratini, E.; Baglioni, P. The two-Yukawa model and its applications: the cases of charged proteins and copolymer micellar solutions. *J. Appl. Crystallogr.* **2007**, *40*, S321−S326.
(57) Liu, Y.; Chen, W. R.; Chen, S. H. Cluster formation in two-Yukawa fluids. *J. Chem. Phys.* **2005**, *122*, 044507.
(58) Kline, S. R. Reduction and analysis of SANS and USANS data using IGOR Pro. *J. Appl. Crystallogr.* **2006**, *39*, 895−900.
(59) Lavoisier, A.; Schlaeppi, J.-M. Early developability screen of therapeutic antibody candidates using Taylor dispersion analysis and UV area imaging detection. *mAbs* **2015**, *7*, 77−83.
(60) Brader, M. L.; Estey, T.; Bai, S.; Alston, R. W.; Lucas, K. K.; Lantz, S.; Landsman, P.; Maloney, K. M. Examination of thermal unfolding and aggregation profiles of a series of developable therapeutic monoclonal antibodies. *Mol. Pharmaceutics* **2015**, *12*, 1005−17.
(61) Thiagarajan, G.; Semple, A.; James, J. K.; Cheung, J. K.; Shameem, M. A comparison of biophysical characterization techniques in predicting monoclonal antibody stability. *MAbs* **2016**, *8*, 1088−97.
(62) Zheng, S.; Qiu, D.; Adams, M.; Li, J.; Mantri, R. V.; Gandhi, R. Investigating the degradation behaviors of a therapeutic monoclonal antibody associated with pH and buffer species. *AAPS PharmSciTech* **2017**, *18*, 42−48.
(63) Majumdar, R.; Manikwar, P.; Hickey, J. M.; Samra, H. S.; Sathish, H. A.; Bishop, S. M.; Middaugh, C. R.; Volkin, D. B.; Weis, D. D. Effects of salts from the Hofmeister series on the conformational stability, aggregation propensity, and local flexibility of an IgG1 monoclonal antibody. *Biochemistry* **2013**, *52*, 3376−89.
(64) Iannuzzi, C.; Irace, G.; Sirangelo, I. Differential effects of glycation on protein aggregation and amyloid formation. *Front. Mol. Biosci.* **2014**, *1*, 9.
(65) Mensink, M. A.; Frijlink, H. W.; van der Voort Maarschalk, K.; Hinrichs, W. L. J. How sugars protect proteins in the solid state and during drying (review): Mechanisms of stabilization in relation to stress conditions. *Eur. J. Pharm. Biopharm.* **2017**, *114*, 288−295.
(66) Baek, Y.; Singh, N.; Arunkumar, A.; Zydney, A. L. Effects of histidine and sucrose on the biophysical properties of a monoclonal antibody. *Pharm. Res.* **2017**, *34*, 629−639.
(67) Arakawa, T.; Timasheff, S. N. Stabilization of protein structure by sugars. *Biochemistry* **1982**, *21*, 6536−44.
(68) Kaushik, J. K.; Bhat, R. Why is trehalose an exceptional protein stabilizer? An analysis of the thermal stability of proteins in the presence of the compatible osmolyte trehalose. *J. Biol. Chem.* **2003**, *278*, 26458−65.
(69) Laue, T. Proximity energies: a framework for understanding concentrated solutions. *J. Mol. Recognit.* **2012**, *25*, 165−173.
(70) Chaturvedi, S. K.; Schuck, P. A reappraisal of sedimentation nonideality coefficients for the analysis of weak interactions of therapeutic proteins. *AAPS J.* **2019**, *21*, 35.
(71) Konarev, P. V.; Volkov, V. V.; Sokolova, A. V.; Koch, M. H. J.; Svergun, D. I. PRIMUS: a Windows PC-based system for small-angle scattering data analysis. *J. Appl. Crystallogr.* **2003**, *36*, 1277−1282.
(72) Franke, D.; Petoukhov, M. V.; Konarev, P. V.; Panjkovich, A.; Tuukkanen, A.; Mertens, H. D. T.; Kikhney, A. G.; Hajizadeh, N. R.; Franklin, J. M.; Jeffries, C. M.; Svergun, D. I. ATSAS 2.8: a comprehensive data analysis suite for small-angle scattering from macromolecular solutions. *J. Appl. Crystallogr.* **2017**, *50*, 1212−1225.
(73) Kanai, S.; Liu, J.; Patapoff, T. W.; Shire, S. J. Reversible self-association of a concentrated monoclonal antibody solution mediated by Fab-Fab interaction that impacts solution viscosity. *J. Pharm. Sci.* **2008**, *97*, 4219−27.
(74) He, F.; Woods, C. E.; Litowski, J. R.; Roschen, L. A.; Gadgil, H. S.; Razinkov, V. I.; Kerwin, B. A. Effect of sugar molecules on the viscosity of high concentration monoclonal antibody solutions. *Pharm. Res.* **2011**, *28*, 1552−60.
(75) Arakawa, T.; Ejima, D.; Tsumoto, K.; Obeyama, N.; Tanaka, Y.; Kita, Y.; Timasheff, S. N. Suppression of protein interactions by arginine: a proposed mechanism of the arginine effects. *Biophys. Chem.* **2007**, *127*, 1−8.
(76) Vagenende, V.; Han, A. X.; Mueller, M.; Trout, B. L. Protein-associated cation clusters in aqueous arginine solutions and their effects on protein stability and size. *ACS Chem. Biol.* **2013**, *8*, 416−22.
(77) Hung, J. J.; Dear, B. J.; Dinin, A. K.; Borwankar, A. U.; Mehta, S. K.; Truskett, T. T.; Johnston, K. P. Improving viscosity and stability of a highly concentrated monoclonal antibody solution with concentrated proline. *Pharm. Res.* **2018**, *35*, 133.
(78) Chen, B. L.; Arakawa, T. Stabilization of recombinant human keratinocyte growth factor by osmolytes and salts. *J. Pharm. Sci.* **1996**, *85*, 419−26.
(79) Costantino, H. R.; Langer, R.; Klibanov, A. M. Aggregation of a lyophilized pharmaceutical protein, recombinant human albumin: effect of moisture and stabilization by excipients. *Nat. Biotechnol.* **1995**, *13*, 493−6.
(80) Hofmeister, F. Zur lehre von der wirkung der salze. *Naunyn-Schmiedeberg's Arch. Pharmacol.* **1888**, *25*, 1−30.
(81) Zhang, Y.; Cremer, P. S. Interactions between macromolecules and ions: The Hofmeister series. *Curr. Opin. Chem. Biol.* **2006**, *10*, 658−63.
(82) Curtis, R.; Lue, L. A molecular approach to bioseparations: Protein-protein and protein-salt interactions. *Chem. Eng. Sci.* **2006**, *61*, 907−923.
(83) Kerlin, R. L.; Li, X. In *Haschek and Rousseaux's Handbook of Toxicologic Pathology*, 3rd ed.; Haschek, W., Rousseaux, C., Wallig, M., Eds.; Academic Press: Boston, 2013; pp 725−750.
(84) Elder, D. P.; Kuentz, M.; Holm, R. Pharmaceutical excipients - quality, regulatory and biopharmaceutical considerations. *Eur. J. Pharm. Sci.* **2016**, *87*, 88−99.
(85) Arakawa, T.; Tsumoto, K. The effects of arginine on refolding of aggregated proteins: not facilitate refolding, but suppress aggregation. *Biochem. Biophys. Res. Commun.* **2003**, *304*, 148−52.
(86) Geng, S. B.; Cheung, J. K.; Narasimhan, C.; Shameem, M.; Tessier, P. M. Improving monoclonal antibody selection and engineering using measurements of colloidal protein interactions. *J. Pharm. Sci.* **2014**, *103*, 3356−3363.
(87) Turner, A.; Schiel, J. E. Qualification of NISTmAb charge heterogeneity control assays. *Anal. Bioanal. Chem.* **2018**, *410*, 2079−2093.
(88) Connolly, B. D.; Petry, C.; Yadav, S.; Demeule, B.; Ciaccio, N.; Moore, J. M. R.; Shire, S. J.; Gokarn, Y. R. Weak interactions govern the viscosity of concentrated antibody solutions: high-throughput analysis using the diffusion interaction parameter. *Biophys. J.* **2012**, *103*, 69−78.
(89) Lehermayr, C.; Mahler, H.-C.; Mäder, K.; Fischer, S. Assessment of net charge and protein-protein interactions of different monoclonal antibodies. *J. Pharm. Sci.* **2011**, *100*, 2551−62.
(90) Saito, S.; Hasegawa, J.; Kobayashi, N.; Kishi, N.; Uchiyama, S.; Fukui, K. Behavior of monoclonal antibodies: relation between the second virial coefficient (B (2)) at low concentrations and aggregation propensity and viscosity at high concentrations. *Pharm. Res.* **2012**, *29*, 397−410.
(91) Jayaraman, J.; Wu, J.; Brunelle, M. C.; Cruz, A. M. M.; Goldberg, D. S.; Lobo, B.; Shah, A.; Tessier, P. M. Plasmonic measurements of

DOI: 10.1021/acs.molpharmaceut.9b00687
Mol. Pharmaceutics 2019, 16, 4319−4338

monoclonal antibody self-association using self-interaction nanoparticle spectroscopy. *Biotechnol. Bioeng.* **2014**, *111*, 1513.
(92) Whitaker, N.; Xiong, J.; Pace, S. E.; Kumar, V.; Middaugh, C. R.; Joshi, S. B.; Volkin, D. B. A formulation development approach to identify and select stable ultra-high-concentration monoclonal antibody formulations with reduced viscosities. *J. Pharm. Sci.* **2017**, *106*, 3230−3241.
(93) Wang, W.; Lilyestrom, W. G.; Hu, Z. Y.; Scherer, T. M. Cluster size and quinary structure determine the rheological effects of antibody self-association at high concentrations. *J. Phys. Chem. B* **2018**, *122*, 2138−2154.
(94) Lilyestrom, W. G.; Yadav, S.; Shire, S. J.; Scherer, T. M. Monoclonal antibody self-association, cluster formation, and rheology at high concentrations. *J. Phys. Chem. B* **2013**, *117*, 6373−84.
(95) Chi, E. Y. *Pharmaceutical Excipients: Properties, Functionality, and Applications in Research and Industry*; Koo, O. M. Y., Ed.; John Wiley and Sons, Ltd, 2016; Chapter 4, pp 145−198.
(96) Buck, P. M.; Chaudhri, A.; Kumar, S.; Singh, S. K. Highly viscous antibody solutions are a consequence of network formation caused by domain-domain electrostatic complementarities: insights from coarse-grained simulations. *Mol. Pharmaceutics* **2015**, *12*, 127−39.
(97) Wang, W.; Nema, S.; Teagarden, D. Protein aggregation−pathways and influencing factors. *Int. J. Pharm.* **2010**, *390*, 89−99.
(98) Thakkar, S. V.; Joshi, S. B.; Jones, M. E.; Sathish, H. A.; Bishop, S. M.; Volkin, D. B.; Middaugh, C. R. Excipients differentially influence the conformational stability and pretransition dynamics of two IgG1 monoclonal antibodies. *J. Pharm. Sci.* **2012**, *101*, 3062−3077.
(99) Fayos, R.; Pons, M.; Millet, O. On the origin of the thermostabilization of proteins induced by sodium phosphate. *J. Am. Chem. Soc.* **2005**, *127*, 9690−9691.
(100) Katayama, D. S.; Nayar, R.; Chou, D. K.; Valente, J. J.; Cooper, J.; Henry, C. S.; Vander Velde, D. G.; Villarete, L.; Liu, C. P.; Manning, M. C. Effect of buffer species on the thermally induced aggregation of interferon-tau. *J. Pharm. Sci.* **2006**, *95*, 1212−26.
(101) Liu, L.; Qi, W.; Schwartz, D. K.; Randolph, T. W.; Carpenter, J. F. The effects of excipients on protein aggregation during agitation: an interfacial shear rheology study. *J. Pharm. Sci.* **2013**, *102*, 2460−70.
(102) Gekko, K.; Koga, S. Increased thermal stability of collagen in the presence of sugars and polyols. *J. Biochem.* **1983**, *94*, 199−205.
(103) Wang, S.; Zhang, N.; Hu, T.; Dai, W.; Feng, X.; Zhang, X.; Qian, F. Viscosity-lowering effect of amino acids and salts on highly concentrated solutions of two IgG1 monoclonal antibodies. *Mol. Pharmaceutics* **2015**, *12*, 4478−87.
(104) Bauer, K. C.; Suhm, S.; Woell, A. K.; Hubbuch, J. Impact of additives on the formation of protein aggregates and viscosity in concentrated protein solutions. *Int. J. Pharm.* **2017**, *516*, 82−90.
(105) Zhang, J.; Frey, V.; Corcoran, M.; Zhang-van Enk, J.; Subramony, J. A. Influence of arginine salts on the thermal stability and aggregation kinetics of monoclonal antibody: dominant role of anions. *Mol. Pharmaceutics* **2016**, *13*, 3362−3369.

DOI: 10.1021/acs.molpharmaceut.9b00687
Mol. Pharmaceutics 2019, 16, 4319−4338